A high throughput screening method for the nano-crystallization of salts of organic cations

Nievergelt, Philipp P ; Babor, Martin ; Čejka, Jan ; Spingler, Bernhard

Abstract: The generation of solid salts of organic molecules is important to the chemical and pharmaceutical industry. Commonly used salt screening methods consume a lot of resources. We employed a combination of ion exchange screening and vapour diffusion for crystallization. This technique is semi-automatic and requires just nanoliters of the solution of the analyte to be crystallized. This high throughput screening yielded single crystals of sufficient size and quality for single-crystal X-ray structure determination using an in-house X-ray diffractometer. The broad scope of our method has been shown by challenging it with 7 very different organic cations, whose aqueous solubilities vary by a factor of almost 1000. At least one crystal structure for 6 out of 7 tested cations was determined; 4 out of the successful 6 ones had never been crystallized before. Our method is extremely attractive for high throughput salt screening, especially for active pharmaceutical ingredients (APIs), as about 40% of all APIs are cationic salts. Additionally, our screening is a new and very promising procedure for the crystallization of salts of organic cations.

DOI: https://doi.org/10.1039/C8SC00783G

Chemical Science

EDGE ARTICLE

Cite this: *Chem. Sci.*, 2018, **9**, 3716

A high throughput screening method for the nano-crystallization of salts of organic cations†

Philipp P. Nievergelt, ‡[a] Martin Babor, ‡[ab] Jan Čejka [b] and Bernhard Spingler *[a]

Received 16th February 2018
Accepted 6th March 2018

DOI: 10.1039/c8sc00783g

rsc.li/chemical-science

The generation of solid salts of organic molecules is important to the chemical and pharmaceutical industry. Commonly used salt screening methods consume a lot of resources. We employed a combination of ion exchange screening and vapour diffusion for crystallization. This technique is semi-automatic and requires just nanoliters of the solution of the analyte to be crystallized. This high throughput screening yielded single crystals of sufficient size and quality for single-crystal X-ray structure determination using an in-house X-ray diffractometer. The broad scope of our method has been shown by challenging it with 7 very different organic cations, whose aqueous solubilities vary by a factor of almost 1000. At least one crystal structure for 6 out of 7 tested cations was determined; 4 out of the successful 6 ones had never been crystallized before. Our method is extremely attractive for high throughput salt screening, especially for active pharmaceutical ingredients (APIs), as about 40% of all APIs are cationic salts. Additionally, our screening is a new and very promising procedure for the crystallization of salts of organic cations.

Introduction

Organic salts are multi-component ionic compounds, in which at least one of the components is an organic ion. The focus of this paper is the organic, cationic part of salts. Different salts of the same organic cation can have significantly different physicochemical properties.[1–6] The critical properties are solubility,[7] crystal shape, hygroscopicity, melting point, and physical as well as chemical stability. The selection of a suitable anion can avoid problems during production, storage or shipping of an organic salt. For example, an appropriate anion can improve the purification and flow properties of the powder and/or reduce the hygroscopicity. Therefore, salt screening is a decisive step during the development and optimization of the production process of an organic salt.[2] It can significantly reduce the production cost of the chemical or pharmaceutical, as about 40% of all active pharmaceutical ingredients (APIs) are cationic salts.[8] However, there are also requirements for an ideal screening. It shall require the least possible amount of material, human work and time. At the same time, it should be as effective as possible in discovering new salts. Additionally, the ability to analyse the new crystalline forms directly from the basic screening would be a great advantage, ideally by single crystal X-ray diffraction (SCXRD) structure analysis, since fast access to SCXRD can save a lot of material and lab work, such as immediately identifying false positive screening hits.

Recently, several innovations have been described that, with the help of crystallography, allow the structure determination of compounds, which had previously been impossible by applying the methods of traditional crystal growth.[9,10] The 'crystalline sponge' method was originally introduced in 2013 by Fujita and co-workers[11] and has further been improved over the last few years.[12,13] This method opened up new possibilities for determining the crystal structures of apolar compounds that are available only in minute amounts. However, this method is a 3 step procedure: (1) synthesis of the MOF host, (2) exchange of the previous solvent by an apolar one, and (3) soaking of the MOF crystal with the analyte. All steps are non-trivial to perform and especially the last step has to be optimized for every single compound. Alternative sponge methods have been described, avoiding the exchange of guest molecules; however, they require more analyte material and synchrotron radiation.[14,15] Even the most recent optimisation of the crystal sponge method is still labour intensive, requires the analyte to be soluble in dichloromethane and can only in exceptional cases be used as an *ab initio* structure determination method without additional knowledge of the analyte.[16] A different MOF lattice has recently been developed by the group of Yaghi for the co-crystallization

[a]*Department of Chemistry, University of Zurich, Winterthurerstr. 190, 8057 Zurich, Switzerland. E-mail: spingler@chem.uzh.ch; Web: http://www.chem.uzh.ch/en/research/groups/spingler.html*

[b]*Department of Solid State Chemistry, University of Chemistry and Technology Prague, Prague 6, 166 28, Czech Republic*

† Electronic supplementary information (ESI) available: Details of experimental, crystallographic procedures and descriptions of the crystal structures. CCDC 1585747–1585765 and 1823199–1823201. For ESI and crystallographic data in CIF or other electronic format see DOI: 10.1039/c8sc00783g

‡ These authors contributed equally to this work.

of carboxylates or alcohol containing molecules.[17] Summarizing the previous developments, a new method that could facilitate the crystallization of cationic, polar compounds would be highly desirable.

Results and discussion

Our new method addresses this need. Our screening technique is based on two simple ideas and combines basic screening with single crystal growth directly followed by structural analysis. The first hypothesis assumes that chloride salts of most cations have the highest solubility in water and analogously that sodium salts are the most common form of salts with a high solubility in water. The second hypothesis supposes that a slow increase of saturation might lead to the growth of single crystals. According to the first idea, if we mix solutions of organic chloride salts with various sodium salts, the least soluble combination of dissolved ions should crystallize, which should be a new organic salt. In addition, the mixture of the starting salts does not have to be equimolar, because all remaining ions will still be dissolved in water. Concerning the second idea, an increase of analyte concentration within a drop is generated by the method of vapour diffusion (see ESI Fig. 1†), which was previously developed for protein crystallization.[18] This method basically consists of mixing 100–500 nl of the analyte in water with the same volume of a crystallization cocktail – in our case this is normally a sodium salt – to generate a small drop of 200–1000 nl volume. The drop is then equilibrated *via* the vapour phase against the big reservoir consisting of only the crystallization cocktail. Since the crystallization cocktail in the drop was diluted with the analyte, the water diffuses *via* the gas phase back to the reservoir. The mixing of the analyte and the sodium salt in the drop might already generate a supersaturated solution, while the diffusion of the water to the reservoir will increase this effect. In order to automate and miniaturize the whole procedure, the pipetting of the reservoir and the drop solutions, as well as the visual monitoring, is carried out by a robot. Such robots are commonly being used in most biochemical laboratories and pharmaceutical companies that are engaged in structural biology projects.

Currently, the salt screening of active pharmaceutical ingredients (APIs) that can be protonated is mainly done by isolating and weighing the free base followed by addition of different acids in various solvents.[19–21] This process is labour intensive and can be unreliable, as some free bases are hygroscopic, prone to oxidation, or may otherwise be chemically unstable. An additional disadvantage of this method is that the ratio of API to acid has a direct influence upon the pH in the chosen solvent and therefore also upon the propensity to crystallize. Furthermore, different solvents might change the degree of protonation of the API. Therefore, the amount of added acid must be chosen carefully in advance for each solvent.

In order to evaluate our new method of crystallization, we chose salts with seven quite different organic cations (Fig. 1). The chosen compounds include permanent cations (due to the presence of tetraalkylated ammonium groups), as well as

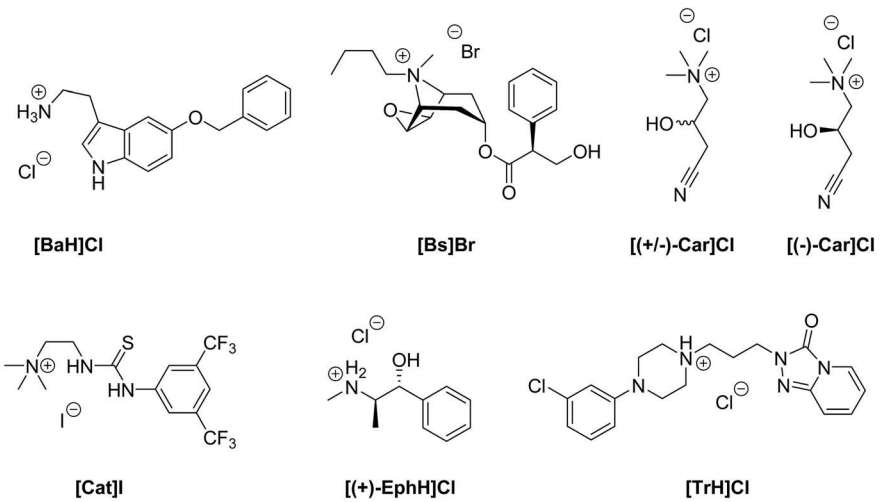

Fig. 1 Selected compounds (5-benzyloxytryptaminium chloride, butyl scopolammonium bromide, (*R*,*S*)-carnitinenitrile chloride, (*R*)-(−)-carnitinenitrile chloride, iodide salt of the catalyst, (1*S*,2*R*)-(+)-ephedrine hydrochloride and trazodone hydrochloride) for crystallization and salt screening.

Table 1 Needed amount of material in milligrams for one 96-well crystallization screening (assuming 100 nl consumption per crystallization drop of a 90% saturated solution plus a 2 μl pipetting reserve for one 96-well plate)

	[BaH]Cl	[Bs]Br	[(+/−)-Car]Cl	[(−)-Car]Cl	[Cat]I	[(+)-EphH]Cl	[TrH]Cl
Amount [mg]	0.026	22	13	16	0.083	3.1	0.46
Aqueous solubility [mg ml^{-1}]	2.2 ± 0.1	1800 ± 200	1120 ± 106	1300 ± 200	6.9 ± 0.1	257 ± 1	38.5 ± 0.2

Table 2 Crystallization results

Source of counterion	Conc. [M]	[BaH]Cl	[Bs]Br	[(+/−)-Car]Cl	[(−)-Car]Cl	[Cat]I	[(+)-EphH]Cl	[TrH]Cl
Sodium chloride	3.00	R.	P. S.			P. S.	D. S.	P. S.
Sodium chloride	1.50	R.				P. S.		P. S.
Sodium bromide	4.00	R.[a]	P. S.		P.	D. S.	D. S.	P. S.
Sodium bromide	2.00	R.[a]	P. S.			P. S.		P. S.
Sodium iodide	5.30	R.	P. S.			P. S.	D. S.[b]	D. S.
Sodium iodide	2.50	R.	P. S.			P. S.		D. S.
Sodium iodide	1.25	R.	P. S.			P. S.		D. S.
Potassium thiocyanate	7.30	D. S.	P. S.		P.	P. S.	P.	P. S.
Potassium thiocyanate	3.50	D. S.	P. S.			P. S.	P.	P. S.
Potassium thiocyanate	1.75	D. S.	P. S.			P. S.	D. S.	P. S.
Sodium dicyanamide	0.70	P.	P. S.			P. S.		P. S.
Sodium tetrafluoroborate	4.00	D. S.	P. S.			P. S.		P. S.
Sodium tetrafluoroborate	2.00	P.	P. S.			P.		P.
Potassium hexafluorophosphate	0.24	P.	P. S.			D. S.	P.	P. S.
Sodium tetraphenylborate	0.40		P.	R.	R.	P.		P.
Sodium tetraphenylborate	0.20		P.	R.	R.	P.	P.	P.
Disodium sulfate	1.00	D. S.						P. S.
Sodium methanesulfonate	3.60	P.	P. S.					P. S.
Sodium methanesulfonate	1.80	P.	P. S.			P. S.		P. S.
Sodium triflate	0.80	P.	P. S.			P.		P. S.
Sodium isethionate	2.20	P.	P. S.					P. S.
Sodium isethionate	1.10	P.						
Sodium (+/−)-camphorsulfonate	2.28							
Sodium benzenesulfonate	0.98	P.						P.
Sodium 3-nitrobenzensulfonate	0.42	P.	P. S.			P. S.		P. S.
Sodium *p*-toluenesulfonate	0.15							P.
Sodium 1-naphthalenesulfonate	0.35	P.	P. S.			P. S.		P. S.
Sodium 2-naphthalenesulfonate	0.13	P.	P. S.			P.		
Disodium 2,6-naphthalenedisulfonate	0.085					P. S.	P.	P.
Sodium nitrate	4.60	P.	P. S.					P. S.
Sodium nitrate	2.30	P.	P. S.			P. S.		P. S.
Sodium benzoate	1.80							
Sodium salicylate	2.20							
Sodium salicylate	1.10		P. S.			P. S.		P. S.
Sodium 4-aminosalicylate dihydrate	1.50	P.						
Sodium *meta*-hydroxybenzoate	1.30							P. S.
Sodium nicotinate	2.96							P. S.
Sodium nicotinate	1.48							P. S.
Potassium hydrogen phthalate	0.27	P.				P. S.		P. S.
Disodium isophthalate	1.40							P. S.
Disodium terephthalate	0.060	P.			P.	P. S.		P. S.
Disodium pamoate	0.050	P.					P. S.	
Sodium formate	6.00	P.	P. S.			P. S.		P. S.
Sodium formate	3.00	P.	P. S.			P. S.		P. S.
Sodium acetate	2.60	P.	P. S.					P. S.
Sodium trifluoroacetate	2.40	P.	P. S.			P. S.		P. S.
Sodium 2-phenylpropionate	1.70	P.				P. S.		
Sodium DL-mandelate	0.25	P.						P. S.
Sodium D-mandelate	0.25	P.				P. S.	P.	P. S.
Sodium L-mandelate	0.25	P.						P. S.
Sodium 1-naphthaleneacetate	0.43	P.					P. S.	
Sodium diphenylacetate	0.33	P.					P. S.	P. S.

Table 2 (*Contd.*)

Sodium *N*-acetylglycinate	2.28	P.	P. S.			P. S.
Sodium hippurate	1.46					
Sodium pyrrolidone carboxylate	4.96		P. S.		P. S.	P. S.
Sodium propionate	5.20	P.	P. S.		P. S.	P. S.
Sodium propionate	2.60	P.				P. S.
Sodium DL-lactate	3.42	P.	P. S.		P. S.	P. S.
Sodium L-lactate	3.42	P.	P. S.		P. S.	P. S.
Sodium pyruvate	3.00	P.	P. S.		P. S.	P. S.
Sodium pyruvate	1.50	P.	P. S.		P. S.	P. S.
Sodium valerate	3.19			P.		P. S.
Sodium hexanoate	2.70					P. S.
Sodium 2-ethylhexanoate	4.20					
Sodium 2-ethylhexanoate	2.10					
Potassium gluconate	1.10	P.				
Sodium octanoate	1.56					
Sodium hydrogen carbonate	0.60	P.		P.		P. S.
Disodium carbonate	1.00	P.		P.		P. S.
Disodium oxalate	0.14	D. S.			D. S.	D. S.
Disodium malonate	2.97	P.	P. S.		P. S.	P. S.
Disodium succinate	1.13	R.[a]	P. S.		P. S.	P. S.
Disodium maleate	0.66	P.			P. S.	P. S.
Disodium fumarate	0.73					
Disodium DL-malate	2.27	P.	P. S.			P. S.
Disodium L-malate	2.92	P.	P. S.			P. S.
Sodium potassium L-tartrate	1.40	D. S.	P. S.			P. S.
Disodium DL-tartrate	0.55	P.	P. S.	F. P.		R.[c]
Disodium L-tartrate	1.00	P.	P. S.		P. S.	P. S.
Disodium (+)-*O*,*O*′-dibenzoyl-D-tartrate	0.26	P.			P. S.	P. S.
Potassium antimony L-tartrate	0.054	D. S.			P.	P. S.
Disodium *N*-acetylglutamate	1.63	P.	P. S.		P. S.	P. S.
Disodium adipate	1.19	P.	P. S.		P. S.	P. S.
Potassium D-saccharate	0.050				P.	
Trisodium citrate dihydrate	0.90	P.	P. S.		P. S.	P. S.
Sodium DL-aspartate	0.25					P. S.
Sodium L-aspartate	0.25					P. S.
Sodium L-glutamate	2.00					P. S.
Sodium L-glutamate	1.00					P. S.
Sodium diethyldithiocarbamate	0.011					P. S.
Sodium saccharine	1.57		P. S.			
Disodium hydrogen phosphate	0.43	P.			P. S.	P. S.
Sodium dihydrogen phosphate	4.00	R.	P. S.			P. S.
Sodium dihydrogen phosphate	2.00	R.	P. S.			P. S.
Disodium citrate	0.93		P. S.			P. S.
Trisodium phosphate dodecahydrate	0.36	P. S.				P. S.

D. S.	Direct structure solution followed by successful refinement of the structure
R.	Structure solution after recrystallization or slightly modified crystallization conditions followed by successful refinement of the structure
P.	Powder sample or too small crystals, without analysis
P. S.	Phase separation
	Clear well
F. P.	False positive

[a]The structure will be described in a following paper.
[b]Grown at 4 °C.
[c]See ESI for more details.

compounds that can be protonated only at lower pH. Their solubilities in water range from 2.2 to 1800 mg ml^{-1} (Table 1). Furthermore, we included a racemic compound to evaluate the potential for enantiomeric resolution by chiral and sometimes even enantiomerically pure anions. Additionally, we tested the corresponding enantiomerically pure compound in order to compare the ease of crystallization of a racemate and of one of its enantiomers. Most of the chosen organic compounds have no reported crystal structure at all, while one, ephedrine, is known to form many different salt forms.[22] 5-Benzyloxytryptaminium chloride (**[BaH]Cl**) is an API, which acts as an antagonist of the TRPM8 ion-channel. It is used for the treatment of prostate cancer or benign prostate hyperplasia.[23] The Cambridge Structural Database (CSD)[24] does not contain any structure of 5-benzyloxytryptamine. Butyl scopolammonium bromide (**[Bs]Br**) is being used to treat crampy abdominal pain, renal colic, and esophageal and bladder spasms. The crystal structure its methanol solvate has been reported.[25] (*R*,*S*)-Carnitinenitrile chloride (**[(+/−)-Car]Cl**) and (*R*)-(−)-carnitinenitrile chloride (**[(−)-Car]Cl**) are being used as intermediates for the preparation of carnitine or derivatives of carnitine, both of which are APIs with many different effects from neurology to diabetes mellitus.[26–28] There is no structure of any carnitinenitrile in the CSD. 2-(3-(3,5-Bis(trifluoromethyl) phenyl)-thioureido)-*N*,*N*,*N*-trimethylethanaminium iodide (**[Cat]I**) is the achiral version of chiral thiourea catalysts,[29] and the former can be used for the aminolysis of *N*-acyl homoserine lactones.[30] No structure of any salt that contains $[Cat]^+$ can be found in the CSD. (1*S*,2*R*)-(+)-Ephedrine hydrochloride (**[(+)-EphH]Cl**) is an active pharmaceutical ingredient used for the treatment of emphysema and bronchial asthma. Many crystal structures have been described for (+)-, (−)- or (+/−)-ephedrine salts.[22,31] Ephedrine was also used as a test case for several salt screening studies.[20,32] Trazodone hydrochloride (**[TrH]Cl**) is a selective inhibitor of serotonin and norepinephrine reuptake in a ratio of 25 : 1, and it is being used pharmaceutically as an antidepressant.[33] Only the crystal structure of trazodone hydrochloride has been reported and can be found in the CSD.[34]

Our method employs a crystallization robot with a setup that is commonly used in protein crystallography, but only exceptionally in small molecule crystallography.[35] Initially, we chose a crystallization setup that consisted of 500 nl of the aqueous nearly saturated solution of the analyte; however repetitions of the crystallizations with just 150 and 100 nl of the analyte solutions were similarly successful. The last measurement series with

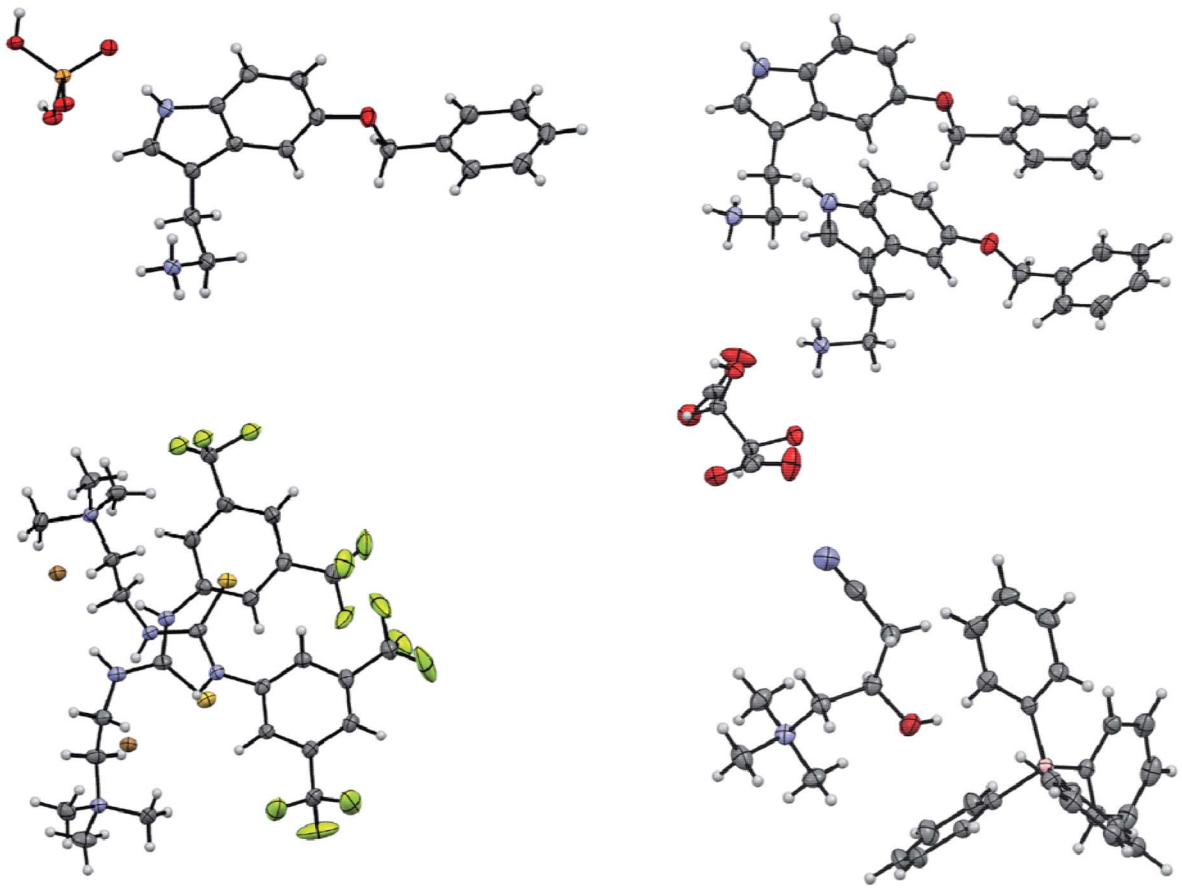

Fig. 2 Displacement ellipsoid representations of the crystal structures of 5-benzyloxytryptaminium dihydrogenphosphate (top left), 5-benzyloxytryptaminium tartrate (minor disordered parts and water molecules omitted for clarity, top right), 2-(3-(3,5-bis(trifluoromethyl) phenyl)-thioureido)-*N*,*N*,*N*-trimethylethanaminium bromide (lower left) and (*R*)-carnitinenitrile tetraphenylborate (lower right). Ellipsoids are drawn at 50% probability.

100 nl analyte solution required really minute amounts of material and still yielded high quality crystals (ESI Fig. 3†) that directly led to publishable structures. As can be seen in Table 1, the required amount essentially depends upon the solubility of the compound in water. For our method, we work with solutions that are 90% saturated. We used two procedures to obtain these solutions: one was to determine the apparent solubility by dissolution of the solid material and observing the progress with a microscope. The other method was much simpler and used less material: we generated a saturated stock solution, separated it from the solid and diluted it then to 90% saturation.

The screening was performed with the seven mentioned organic salts and mainly sodium salts of 77 different counterions (Table 2 and ESI†). The criteria for the selection of the counterions were a known propensity to crystallize and/or being a compound that is Generally Recognized As Safe (GRAS)[36] for a potential later use in an API. Each of the chosen 7 analytes was screened under 96 conditions, as some of the counterions were present in the screening at multiple, different concentrations. The screening was stopped after 16 days; however longer equilibration times could be applied. Quite often the crystals formed after a few days, see *e.g.* the case of 5-benzyloxytryptaminium antimony-L-tartrate, in which a change of crystal morphology could be observed (ESI Fig. 2†). The same crystals could sometimes be observed in several drops containing the same counterion at different concentrations. It was possible to determine 15 high quality single crystal structures of chemically different salts directly from the screening without the need for any further optimisation, and 14 of them were novel structures. Additionally, 14 lead hits consisting of too small crystals were manually recrystallized, which yielded in 7 cases big enough crystals that could be measured and refined by SCXRD to give 7 novel structures (Fig. 2 and Table 2). In one further case, covering the drop with oil induced the crystal growth of the free base trazodone. The crystal nucleated at the oil/water interface and then grew by penetrating into the oil. The three compounds – **[Bs]Br**, **[(+/−)-Car]Cl** and **[(−)-Car]Cl** – all having an unusually high solubility of more than one gram per milliliter were most challenging; obviously if the chloride is already present at such high concentrations, it is difficult to substitute it during crystallization from a mixed chloride/anion solution.

Conclusion

Our screening method for the growth of single crystals containing organic cations was very effective: six out of seven tested cationic moieties yielded at least one crystal structure. Also, the primary screening used just a very small amount of material (12 μl of a 90% saturated aqueous solution of a salt with an organic cation) in order to test a total of 96 different conditions, and we were able to determine at least one unit cell directly in most of the positive crystalline hits using in-house X-ray diffractometers. Furthermore, the required manual work is quite low due to the usage of a pipetting robot and a crystal farm, both of which are available in many biochemical institutes and pharmaceutical companies. With just 26 μg of one organic salt employing 100 nl of analyte solution per crystallization experiment, we were able to directly determine the structure of 6 different salts and obtained the lead to another 5 salts. The new screening method requires compounds that can form stable cations in water and have a water solubility of at least 2 mg ml^{-1} of their salt form. We are currently working on a system, which can crystallize less water soluble cations. In contrast to the report of Berghausen,[21] we were able to perform a salt screening with highly water soluble compounds in a purely aqueous environment. Performing the screening at temperatures other than room temperature is possible and yielded a second, unknown polymorph of enantiomerically pure ephedrinium iodide.

Conflicts of interest

There are no conflicts of interest to declare.

Acknowledgements

We thank Prof. Dr Mario Waser for kindly providing compound **[Cat]I**, Lonza Ltd. Basel for providing the sodium dicyanamide, and Beat Blattmann as well as Céline Stutz for setting up our crystallization trials on the robot. We thank Mohammad Al-Qatanani for determining the aqueous solubility of various compounds by HPLC and Prof. Dr Anthony Linden for a critical reading of the manuscript. We thank the University of Zürich, the R'Equip programme of the Swiss National Science Foundation (project number 206021_164018) and the Czech Science Foundation (grant No. 16-10035S) for financial support.

References

1 M. von Raumer, J. Dannappel and R. Hilfiker, *Chem. Today*, 2006, **24**, 41–44.
2 L. Kumar, A. Amin and A. K. Bansal, *Drug Discovery Today*, 2007, **12**, 1046–1053.
3 W.-Q. Tong, in *Developing Solid Oral Dosage Forms*, ed. Y. Chen, G. G. Z. Zhang, L. Liu and W. R. Porter, Academic Press, San Diego, 2009, ch. 4, pp. 75–86.
4 N. Wyttenbach, B. Sutter and P. Hidber, in *Handbook of Pharmaceutical Salts*, ed. P. H. Stahl and C. G. Wermuth, Verlag Helvetica Chimica Acta, 2nd edn., 2011, ch. 8, pp. 203–233.
5 *Pharmaceutical Salts and Co-crystals*, ed. J. Wouters and L. Quéré, Royal Society of Chemistry, Cambridge, 2011.
6 S. R. Byrn, G. Zografi and X. Chen, *J. Pharm. Sci.*, 2010, **99**, 3665–3675.
7 D. P. Elder, R. Holm and H. L. de Diego, *Int. J. Pharm.*, 2013, **453**, 88–100.
8 G. S. Paulekuhn, J. B. Dressman and C. Saal, *J. Med. Chem.*, 2007, **50**, 6665–6672.
9 B. Spingler, S. Schnidrig, T. Todorova and F. Wild, *CrystEngComm*, 2012, **14**, 751–757.
10 P. P. Nievergelt and B. Spingler, *CrystEngComm*, 2017, **19**, 142–147.
11 Y. Inokuma, S. Yoshioka, J. Ariyoshi, T. Arai, Y. Hitora, K. Takada, S. Matsunaga, K. Rissanen and M. Fujita, *Nature*, 2013, **495**, 461–466.

12 Y. Inokuma, S. Yoshioka, J. Ariyoshi, T. Arai and M. Fujita, *Nat. Protoc.*, 2014, **9**, 246–252.
13 M. Hoshino, A. Khutia, H. Xing, Y. Inokuma and M. Fujita, *IUCrJ*, 2016, **3**, 139–151.
14 T. R. Ramadhar, S.-L. Zheng, Y.-S. Chen and J. Clardy, *Acta Crystallogr., Sect. A: Found. Adv.*, 2015, **71**, 46–58.
15 T. R. Ramadhar, S.-L. Zheng, Y.-S. Chen and J. Clardy, *CrystEngComm*, 2017, **19**, 4528–4534.
16 F. Sakurai, A. Khutia, T. Kikuchi and M. Fujita, *Chem.–Eur. J.*, 2017, **23**, 15035–15040.
17 S. Lee, E. A. Kapustin and O. M. Yaghi, *Science*, 2016, **353**, 808–811.
18 A. McPherson and J. A. Gavira, *Acta Crystallogr., Sect. F: Struct. Biol. Commun.*, 2014, **70**, 2–20.
19 B. M. Collman, J. M. Miller, C. Seadeek, J. A. Stambek and A. C. Blackburn, *Drug Dev. Ind. Pharm.*, 2013, **39**, 29–38.
20 M. R. Thorson, S. Goyal, B. R. Schudel, C. F. Zukoski, G. G. Z. Zhang, Y. C. Gong and P. J. A. Kenis, *Lab Chip*, 2011, **11**, 3829–3837.
21 P. B. Tarsa, C. S. Towler, G. Woollam and J. Berghausen, *Eur. J. Pharm. Sci.*, 2010, **41**, 23–30.
22 E. A. Collier, R. J. Davey, S. N. Black and R. J. Roberts, *Acta Crystallogr., Sect. B: Struct. Sci.*, 2006, **62**, 498–505.
23 J. DeFalco, D. Steiger, M. Dourado, D. Emerling and M. A. J. Duncton, *Bioorg. Med. Chem. Lett.*, 2010, **20**, 7076–7079.
24 C. R. Groom, I. J. Bruno, M. P. Lightfoot and S. C. Ward, *Acta Crystallogr., Sect. B: Struct. Sci., Cryst. Eng. Mater.*, 2016, **72**, 171–179.
25 J. M. Leger, M. Gadret and A. Carpy, *Acta Crystallogr., Sect. B: Struct. Crystallogr. Cryst. Chem.*, 1978, **34**, 3705–3709.
26 H. Puetter, E. Roske and H. J. Pander, German Pat., DE3419723A1, 1985.
27 K. Nakayama, H. Honda, Y. Ogawa, T. Ohta and T. Ozawa, US Pat., US5041375, 1991.
28 M. Malaguarnera, *Curr. Opin. Gastroenterol.*, 2012, **28**, 166–176.
29 M. Tiffner, J. Novacek, A. Busillo, K. Gratzer, A. Massa and M. Waser, *RSC Adv.*, 2015, **5**, 78941–78949.
30 M. A. Bertucci, S. J. Lee and M. R. Gagné, *Chem. Commun.*, 2013, **49**, 2055–2057.
31 H. Wu, A. R. West, M. Vickers, D. C. Apperley and A. G. Jones, *Chem. Eng. Sci.*, 2012, **77**, 47–56.
32 S. N. Black, E. A. Collier, R. J. Davey and R. J. Roberts, *J. Pharm. Sci.*, 2007, **96**, 1053–1068.
33 G. Davidoff, M. Guarracini, E. Roth, J. Sliwa and G. Yarkony, *Pain*, 1987, **29**, 151–161.
34 J. P. Fillers and S. W. Hawkinson, *Acta Crystallogr., Sect. B: Struct. Crystallogr. Cryst. Chem.*, 1979, **35**, 498–500.
35 P. K. Mandal, B. Kauffmann, H. Destecroix, Y. Ferrand, A. P. Davis and I. Huc, *Chem. Commun.*, 2016, **52**, 9355–9358.
36 SCOGS (Select Committee on GRAS Substances), https://www.accessdata.fda.gov/scripts/fdcc/?set=SCOGS, accessed 23rd October 2017.

Electronic supplementary information for

A high throughput screening method for the nano-crystallization of salts of organic cations

Philipp P. Nievergelt, Martin Babor, Jan Čejka, Bernhard Spingler*

*Corresponding author: spingler@chem.uzh.ch

Content:

1. Materials and Methods:

1.1. Chemicals

5-benzyloxytryptamine hydrochloride (**[BaH]Cl**) was obtained from Acros Organics, Geel, Belgium. N-Butylscopolammonium bromide (also described as butylscopolamine bromide or hyoscine butylbromide **[Bs]Br**), (1*S*,2*R*)-(+)-ephedrine hydrochloride (**[(+)-EphH]Cl**) and trazodone hydrochloride (**[TrH]Cl**) were obtained from Sigma Aldrich. (*R*,*S*)-carnitinenitrile chloride (**[(+/-)-Car]Cl**) was obtained from Frontier Scientific, Logan, UT, USA. (*R*)-carnitinenitrile chloride (**[(-)-Car]Cl**) was obtained from Angene Chemical, Hong Kong, HK. 2-(3-(3,5-bis(trifluoromethyl)phenyl)thioureido)-N,N,N-trimethylethanammonium iodide (**[Cat]I**) was kindly provided by Prof. Dr. Mario Waser, Linz, Austria; it was prepared analogously as described in [1]. The used water was doubly distilled. Sodium or potassium salts of counterions (SCI) were obtained from various commercial suppliers. If the sodium or potassium salts were not commercially available, the corresponding sodium salts were prepared by titration of the corresponding acids with a hydroxide sodium solution (2 M) until the pH reached 7. The solutions of newly prepared salts were concentrated with the help of a rotary evaporator and dried by lyophilisation at 0.02 mbar. The water content was determined by elemental analysis (carbon, hydrogen and nitrogen) of the salt.

1.2. Stock Solutions

The stock solutions of (*R*,*S*)-carnitinenitrile chloride, (*R*)-carnitinenitrile chloride, (1*S*,2*R*)-(+)-ephedrine hydrochloride, trazodone hydrochloride and iodide catalyst were employed at 90% concentration of the saturated solutions. The approximate solubilities of (*R*,*S*)- and (*R*)-carnitinenitrile chloride were determined by slowly dissolving solid material in water in steps of 10 µl with intense stirring until a clear solution was observed under a microscope (see Supplementary Table 1).

Supplementary Table 1: Determination of apparent solubility of butylscopolamine bromide, carnitinenitrile chloride and trazodone hydrochloride by the dissolution method.

	m [mg]	Last step [µl]	Total volume [µl]	Approximate apparent solubility [mg / ml]
butylscopolamine bromide	158	10	90	1800 ± 200
(*R*,*S*)-carnitinenitrile chloride	78	10	70	1120 ± 160
(*R*)-carnitinenitrile chloride	76	10	60	1300 ± 200
trazodone hydrochloride	10	10	260	38.5 ± 0.2

[Cat]I (5 mg), trazodone hydrochloride (35 mg) and 5-benzyloxytryptamine hydrochloride **[BaH]Cl** (20 mg) were each suspended in water (1 ml). The suspensions were stirred at 22°C for 1 day, centrifuged and filtered through a sterile filter with a pore size of 0.20 µm to yield saturated solutions. Those were finally diluted with water in a volume ratio of 90:10 to yield 90% saturated solutions. The solubility of **[BaH]Cl**, **[Cat]I** and **[EphH]Cl** were determined by precisely weighing about 1 mg of material and dissolving it in a defined volume of a 1:1 mixture of water and methanol (just water for **[EphH]Cl**). With this stock solution, a calibration curve in a HPLC system was generated. The saturated aqueous solution was generated as described before, isolated and diluted ten-fold. The concentration of this solution was determined by HPLC using the previously generated calibration curve. The so determined solubilities were 2.2 ± 0.1 mg / ml for **[BaH]Cl**, 6.9 ± 0.1 mg / ml for **[Cat]I** and 257 ± 1 mg / ml for **[EphH]Cl** in water at 22°C.

The concentrations of stock solutions of the sodium or potassium salts of counterions (SCI) were chosen such as that they were approximately half-saturated. For some highly soluble SCI, additional solutions were generated with lower concentrations. All stock solutions were filtered through sterile filters with a pore size of 0.20 µm. Solubility data were taken from the literature or determined experimentally. The approximate experimental solubility of the sodium or potassium SCI was determined at 22°C by slowly dissolving solid material (between 20 - 200 mg) in water (in steps of 10 - 20 µl) with intense stirring till a clear solution was observed under a microscope. The final concentration was calculated after the volume change of solutions caused by dissolving the solid salts was taken into consideration. Unfortunately, a few salts have some inappropriate physico-chemical properties and we had to use different approaches for preparing the stock solutions.

Disodium DL-tartrate is too hygroscopic to be isolated. A saturated solution was prepared (stirring the suspension for 48 h at 22°C) and this solution was diluted to 50%. The approximate molarity was calculated based on weight change (0.106 g) after drying in a rotary evaporator of 1 ml 50% solution (5 hours, 60 °C and 68 mbar). The calculation of molarity was made with the molar mass of anhydrous disodium DL-tartrate (194.051 g/mol).

Sodium pyrrolidone carboxylate, sodium hexanoate, sodium 2-ethylhexanoate and sodium octanoate all produce gels. Suitable viscous solutions of these salts were used like stock solutions. Sodium pyrrolidone carboxylate cannot be isolated as a powder due to its high hygroscopicity and approximate molarity was calculated based on weight change (0.749 g) after drying in the rotary evaporator 1 ml of the stock solution (5 hours, 60 °C and 68 mbar). The calculation of molarity was made with the molar mass of the anhydrous sodium pyrrolidone carboxylate (151.11 g/mol).

Sodium DL-lactate and sodium L-lactate both produce gels. Solutions of sodium DL-lactate and sodium L-lactate were prepared with a concentration of 30% m (salt) / m (water) based on the concentration of commercially available solutions (50% solution).

1.3. Crystallization of Compounds

The principle of the vapour diffusion [2] is shown in Supplementary Fig. 1. The crystallization screening experiments were performed with the help of the Gryphon LCP nano-drop handler from Art Robbins Instruments in ARI Intelli-Plates 96-3 LVR. 100 - 500 nl of a stock solution of the to be crystallized cation were mixed with the same volume of the stock solutions of the SCI and equilibrated against 75 µl of the stock solution of the same SCI. Each cation was tested for crystallization in 96 wells, each well containing a different condition, and with 77 different SCI in total. Due to the high viscosity of some solutions, all pipetting was done with slow speed. Plates were incubated for 5 - 16 days at 20°C. At the beginning of the study, some plates were additionally incubated at 4°C. The Rock Imager 1000 took a picture of each well with normal light (immediately after setting up the plate and then after 2, 5, 10 and 16 days) and cross polarized light (immediately after setting up the plate and then after 5, 10 and 16 days) (see Supplementary Fig. 2).

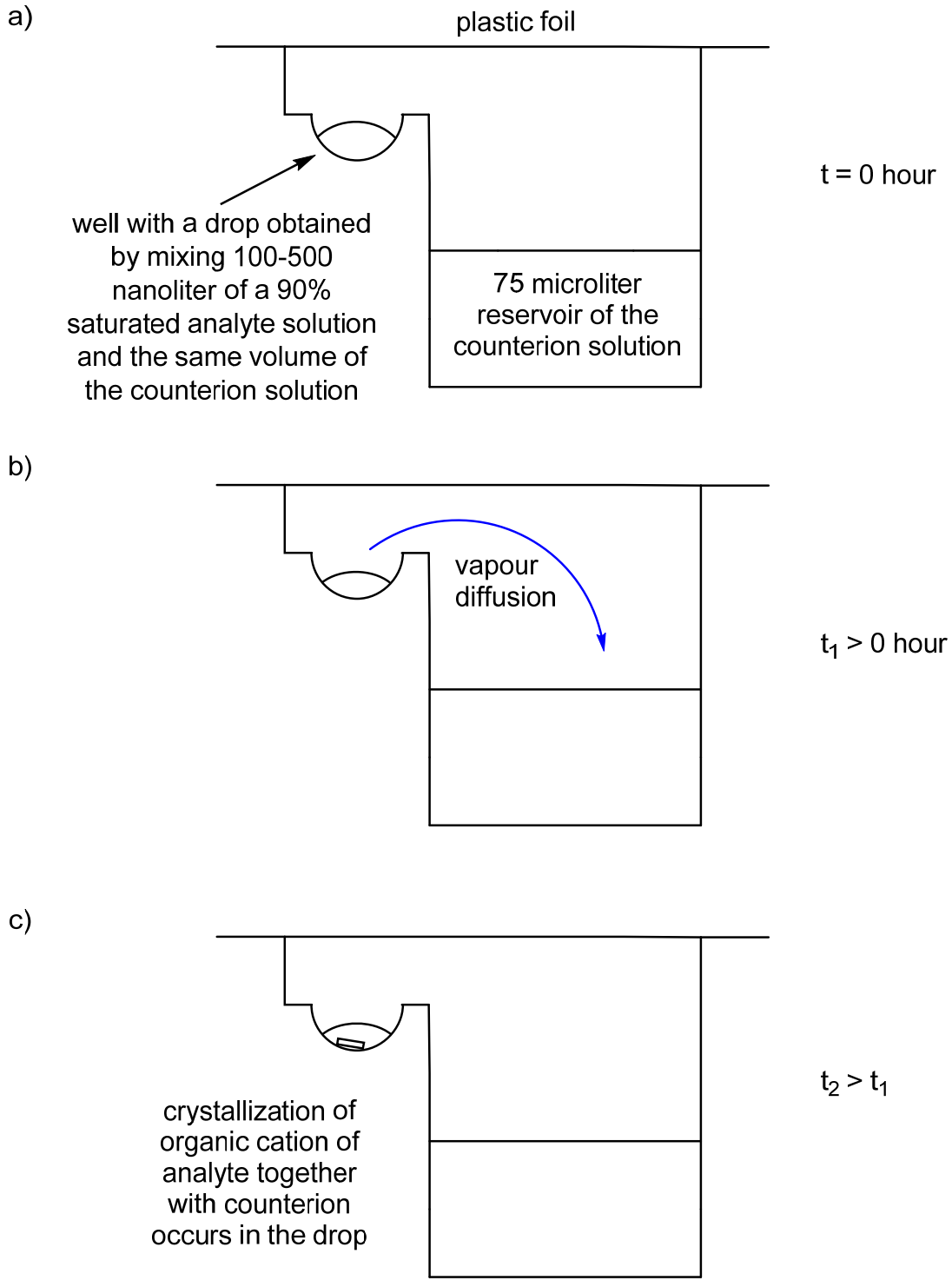

Supplementary Figure 1: Adopted vapour diffusion technique for the crystallization of organic cations.

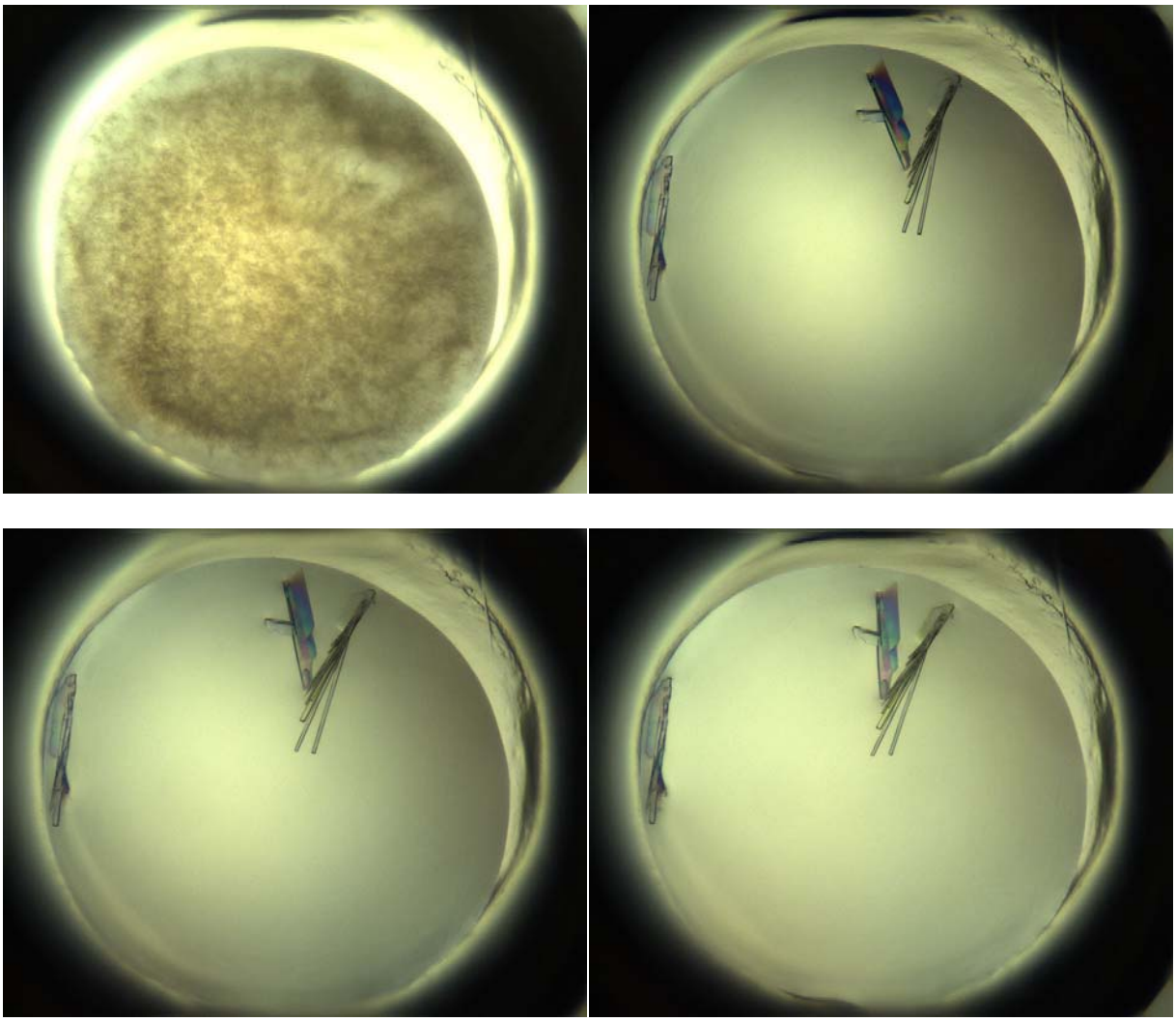

Supplementary Figure 2: Pictures of the crystallization of 5-benzyloxytryptaminium antimony-L-tartrate from 5-benzyloxytryptaminium chloride and potassium antimony-L-tartrate (500 nl each). Pictures shown were taken immediately after setting up the plate (top left) and then after 2 (top right), 5 (bottom left) and 16 (bottom right) days.

If single crystals were observed during this incubation period, they were removed from the wells. In order to do so, wells with formed crystals were opened with a razor blade. Sometimes, the contents of the wells were then covered with oil (Infineum V8512, formerly known as Paratone N). The crystals were fished out with a nylon loop mounted on top of a CrystalCap Magnetic™ (Hampton Research), prepared on a glass slide under oil (Infineum V8512) and measured on a single crystal X-ray diffractometer. The quality of some crystalline material was too poor for structure determination by X-ray single crystal diffraction. These hits were then manually re-synthesized and re-crystallized to obtain better crystals.

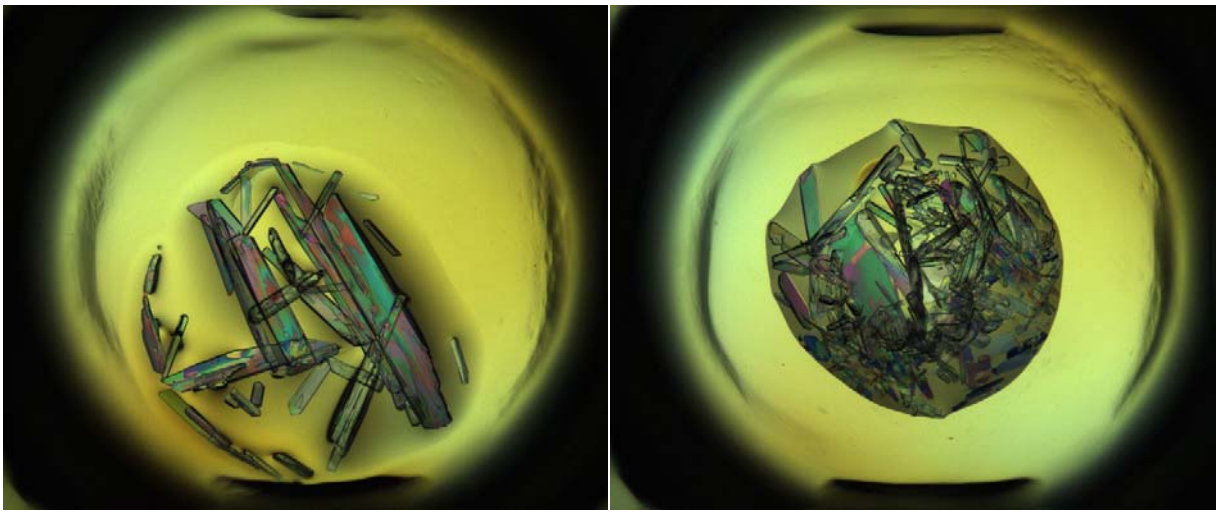

Supplementary Figure 3: Pictures of the crystallization of ephedrine hydrobromide (left) from ephedrine hydrochloride and sodium bromide (100 nl each) and ephedrinium thiocyanide (right) from ephedrine hydrochloride and sodium thiocyanate (100 nl each). Pictures shown were taken after 5 days.

1.4. X-ray Single Crystal Diffraction

Single-crystal X-ray diffraction was measured on two diffractometers. The first one was a Rigaku-Oxford Diffraction XtaLAB Synergy-S dual source diffractometer: Kappa-axis four-circle goniometer with a Dectris Pilatus3 R 200K HPC (Hybrid Photon Counting) detector and Cu and Mo PhotonJet microfocus X-ray sources. The second one was a SuperNova dual source diffractometer: Kappa-axis four-circle goniometer with an Atlas electronic CCD area detector and Cu and Mo microfocus X-ray sources. Computing of measuring strategy and data reduction were performed with *CrysAlis*^{Pro} [3]. The structures were solved with direct methods using *SIR97* [4] or the charge flipping method using *Superflip* [5]. The structures were refined by full-matrix least-squares methods on F^2 with *SHELXL-2014* [6] using the GUI *ShelXle* [7] or refined by least-squares methods on F^2 with *CRYSTALS* [8]. Graphical output was produced with the help of the program *Mercury* [9]. CCDC 1585747-1585765 and 1823199-1823201 contain the Supplementary crystallographic data for this paper. These data can be obtained free of charge from The Cambridge Crystallographic Data Centre via www.ccdc.cam.ac.uk/structures.

2. Description of the structures

[5-benzyloxytryptaminium][chloride]

Crystalline material was obtained from the screening (from a drop containing 500 nl of a 3.0 M sodium chloride and 500 nl of a 90% saturated 5-benzyloxytryptamine hydrochloride solution equilibrating against a reservoir of 3 M sodium chloride, as well as from a drop containing 500 nl of a 1.5 M sodium chloride and 500 nl of a 90% saturated 5-benzyloxytryptamine hydrochloride solution equilibrating against a reservoir of 1.5 M sodium chloride). The quality of the crystals from both experiments was too low for structure determination by SCXRD. The crystal used for SCXRD was crystallized from a mixture of 20 µl of 3 M sodium chloride in water, 20 µl of a 90% saturated solution of 5-benzyloxytryptamine hydrochloride in water and 80 µl acetone. The crystallization technique was slow evaporation in an 1.5 ml Eppendorf vial. This complex crystallized in the monoclinic space group $P2_1/c$. The asymmetric unit consists of one 5-benzyloxytryptaminium cation, which is protonated at the amino group, and one chloride anion. The amino group makes three weak hydrogen bonds to three chloride anions (N1-H11 Cl21(x,1-y,-z): 3.1834(16) Å; N1-H12 Cl21(x,1/2-y,1/2+z): 3.2310(15); N1-H13 Cl21(x,y,1+z): 3.1470(15) Å).

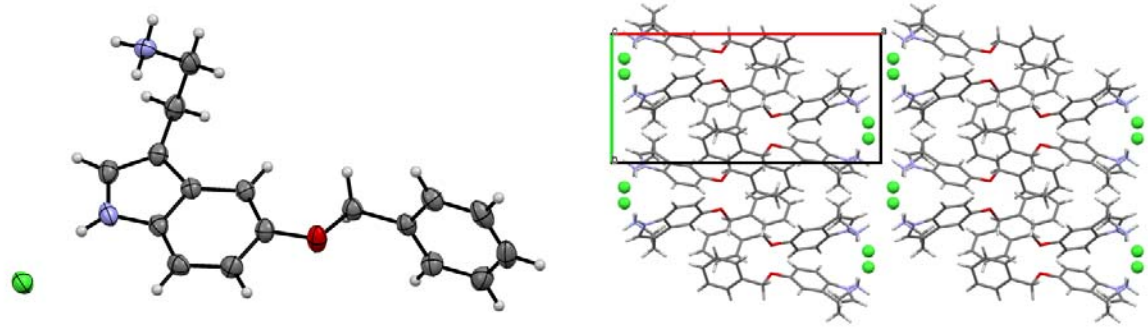

Supplementary Figure 4: Left: displacement ellipsoid representation of **[BaH]Cl**, ellipsoids are drawn at 50% probability. Right: packing diagram of **[BaH]Cl**.

[5-benzyloxytryptaminium][iodide]

Crystalline material was obtained from several crystallization setups: in one case, the drop obtained by mixing 500 nl of a 2.65 M sodium iodide and 500 nl of a 90% saturated 5-benzyloxytryptamine hydrochloride solution was equilibrated against a reservoir of 2.65 M sodium iodide. In two other setups, half and quarter concentrations of iodide in drops and reservoirs respectively were used. All these

conditions gave crystals, but their quality was too low for structure determination by SCXRD. The crystal used for SCXRD was crystallized from a mixture of 20 µl of 5.3 M sodium iodide in water, 20 µl of a 90% saturated solution of 5-benzyloxytryptamine hydrochloride in water and 80 µl acetone. The crystallization technique was slow evaporation. This complex crystallized in the monoclinic space group $P2_1/c$. The asymmetric unit consists of one 5-benzyloxytryptamininum cation, which is protonated at the amino group, and an iodide counterion. The amino group forms three hydrogen bonds to iodide ion (N1-H1 I21(-x,-1/2+y,1/2-z): 3.507(2) Å; N1-H12 I21: 3.562(2) Å; N1-H13 I21(x,3/2-y,1/2+z): 3.526(2) Å).

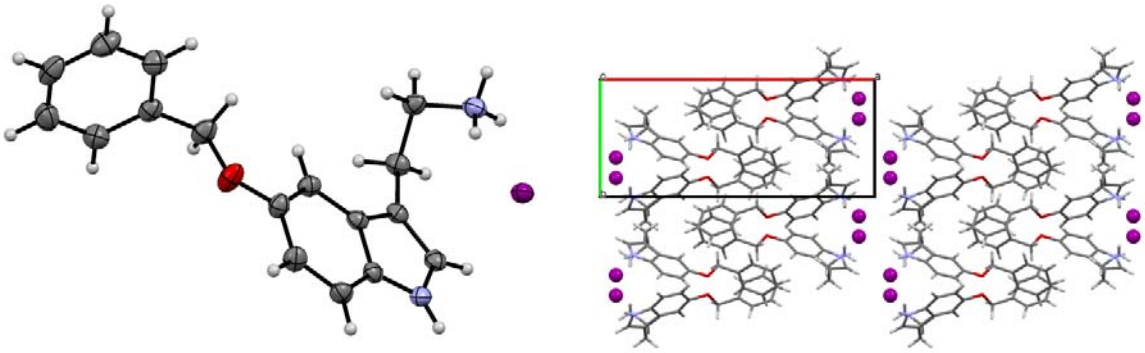

Supplementary Figure 5: Left: displacement ellipsoid representation of **[BaH]I**, ellipsoids are drawn at 50% probability. Right: packing diagram of **[BaH]I**.

[5-benzyloxytryptaminium][dihydrogen phosphate]

The crystalline material, which was obtained directly from the screening, was of insufficient quality for structure determination by SCXRD. The setup was either a drop obtained by mixing 500 nl of a 4 M sodium dihydrogen phosphate solution and 500 nl of a 90% saturated 5-benzyloxytryptamine hydrochloride solution that was equilibrated against a reservoir of 4 M sodium dihydrogen phosphate, or the same setup with half the sodium dihydrogen phosphate concentration. The crystal used for SCXRD was crystallized from a mixture of 20 µl of 4 M sodium dihydrogen phosphate in water, 20 µl of a 90% saturated solution of 5-benzyloxytryptamine hydrochloride in water and 80 µl acetone. The crystallization technique was slow evaporation. This complex crystallized in the monoclinic space group $P2_1/c$. The asymmetric unit consists of one 5-benzyloxytryptaminium cation, which is protonated at the amino group, and a dihydrogen phosphate anion. The amino group forms three hydrogen bonds to oxygen atoms of dihydrogen phosphate (N1-H11 O22(x,3/2-y,-1/2+z): 3.2040(15) Å; N1-H13 O22: 2.9143(14) Å; N1-H12 O24(2-x,1-y,1-z): 2.7683(15) Å). The nitrogen of the indole creates a hydrogen bond to the oxygen atom of the dihydrogen phosphate (N6-H61 O22: 2.9143(14) Å).

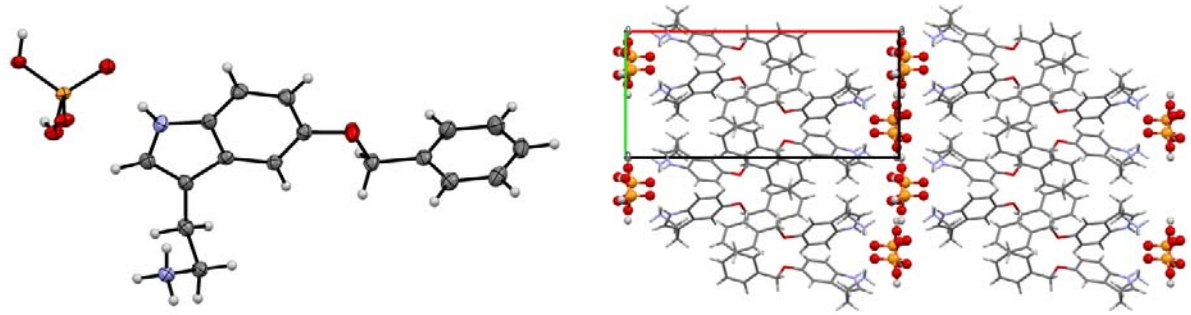

Supplementary Figure 6: Left: displacement ellipsoid representation of **[BaH]H_2PO_4**, ellipsoids are drawn at 50% probability. Right: packing diagram of **[BaH]H_2PO_4**.

[5-benzyloxytryptaminium]$_2$[antimony L-tartrate]·2(H_2O)

This crystal arose in a drop obtained by mixing 500 nl of a 54 mM potassium antimony L-tartrate and 500 nl of a 90% saturated 5-benzyloxytryptamine hydrochloride solution, and equilibrating against a reservoir of 54 mM potassium antimony L-tartrate. This complex crystallized in the monoclinic space group *C*2. The asymmetric unit consists of half an antimony L-tartrate anion, one water molecule and one 5-benzyloxytryptaminium cation, which is protonated at the amino group. The antimony L-tartrate lies on a two-fold axis. The amino group makes three hydrogen bonds to the antimony L-tartrate (N1-H12 O24: 2.960(6) Å, N1-H13 O25(x,1+y,z): 2.983(5) Å and N1-H13 O31(x,1+y,z): 3.003(6) Å).

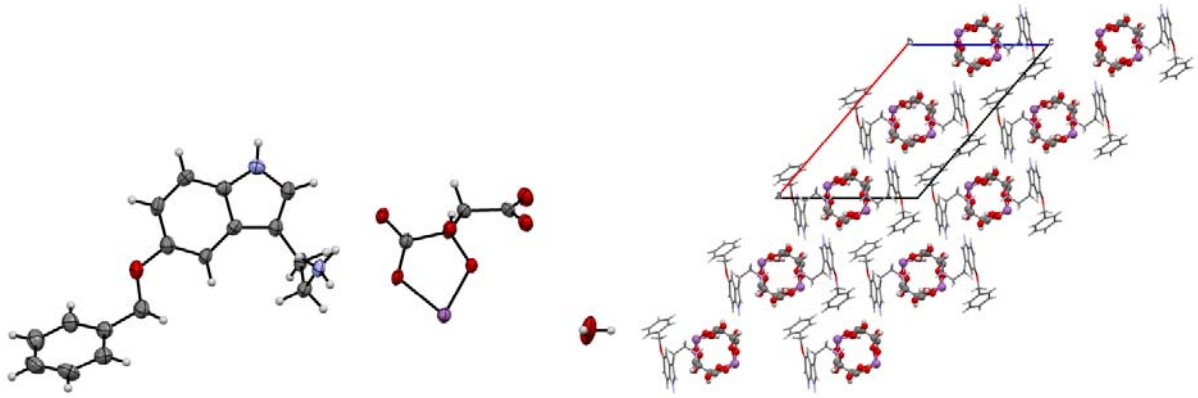

Supplementary Figure 7: Left: displacement ellipsoid representation of **[BaH]$_2$[antimony L-tartrate]·2(H_2O)**, ellipsoids are drawn at 50% probability, for clarity only the asymmetric unit is shown. Right: packing diagram of **[BaH]$_2$[antimony L-tartrate]·2(H_2O)**.

[5-benzyloxytryptaminium]$_2$[L-tartrate]·3.35(H_2O)

This crystal was isolated from a drop obtained by mixing of 500 nl of a 1.4 M sodium potassium L-tartrate and 500 nl of a 90% saturated 5-benzyloxytryptamine hydrochloride solution, and equilibrating against a reservoir of 1.4 M sodium potassium L-tartrate. The salt crystallized in the chiral space group $P2_1$. In the asymmetric unit, there are two 5-benzyloxytryptaminium cations, one tartrate dianion and 3.35 water molecules. The ethylammonium group of one cation is disordered in a ratio of 70:30. The non-disordered ammonium group creates two hydrogen bonds to two carboxylate groups and one fully occupied water molecule. The disordered ammonium group forms two hydrogen bonds to two alcohol groups of one tartrate and one fully occupied water molecule. Because of the disorder, the hydrogen bonding pattern is not discussed in further detail.

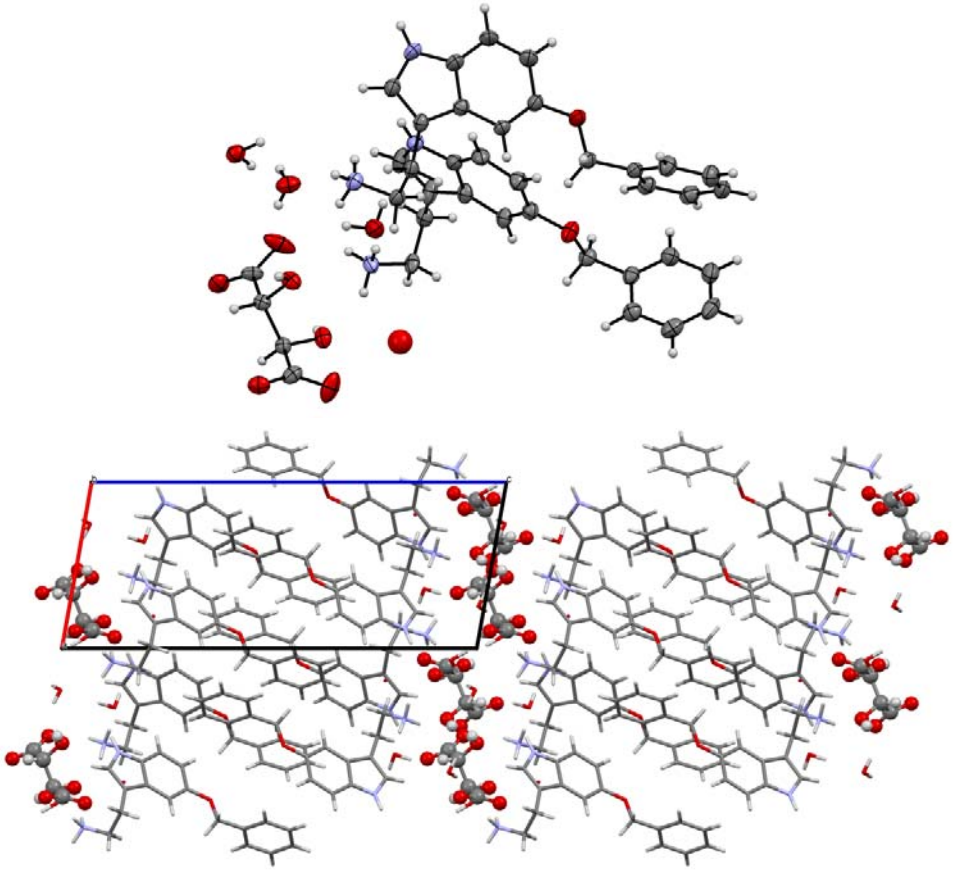

Supplementary Figure 8: Top: displacement ellipsoid representation of **[BaH]$_2$[L-tartrate]·3.35(H_2O)**, ellipsoids are drawn at 50% probability. Only the major conformer of the disordered ethylammonium group is shown for clarity. Below: packing diagram of **[BaH]$_2$[L-tartrate]·3.35(H_2O)**.

[5-benzyloxytryptaminium]$_2$[oxalate]·2(H_2O)

This crystal was isolated from a drop obtained by mixing of 500 nl of a 140 mM disodium oxalate and 500 nl of a 90% saturated 5-benzyloxytryptamine hydrochloride solution, and equilibrating against a reservoir of 140 mM disodium oxalate. This complex crystallized in the monoclinic space group $P2_1$. Refinement in $P2_1/c$ yielded a model with a very high R value and high residual electron densities at irregular positions, hence, the final refinement was carried out in the non-isomorphic subgroup $P2_1$. The asymmetric unit consists of two 5-benzyloxytryptaminium cations, which are protonated at the amino position, one oxalate anion and two water molecules. The two water molecules as well as the oxalate anion are disordered in a ratio of 88:12. Both amino groups form 3 hydrogen bonds. The following discussion concentrates on the major component of the disorder: one ammonium (N1) group binds via two hydrogen bonds to two oxygen atoms of the oxalate (N1-H11 O43(-1+x,y,z): 2.718(2) Å and N1-H11 O41(-x,1/2+y,1-z): 2.801(3) Å) and one to water molecule (N1-H11 O47(-x,-1/2+y,1-z): 2.974(2) Å). The second ammonium (N21) makes one hydrogen bond to the oxygen atom of the oxalate (N21-H211 O45 2.926(3) Å and to two water molecules (N21-H211 O46(-x,1/2+y,1-z): 2.800(2) Å and N21-H211 O48: 2.860(3) Å). One indole group forms a hydrogen bond to the oxygen atom of the oxalate (N6-H61 O43 2.906(2) Å). The second indole group creates a hydrogen bond to a water molecule (N26-H261 O47(1-x,-1/2+y,1-z): 2.976(2) Å).

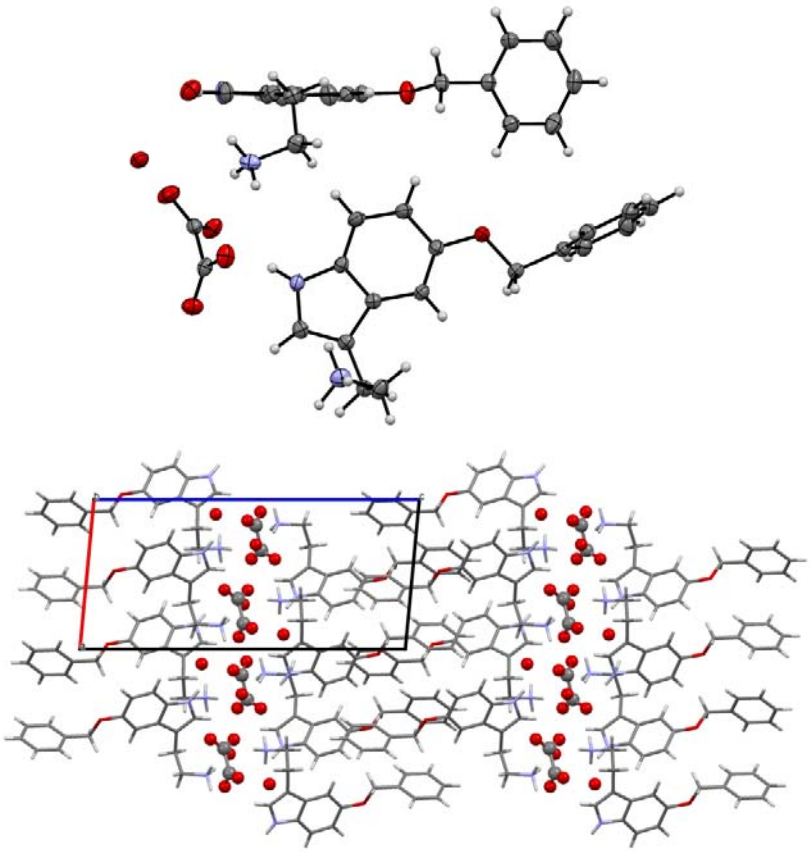

Supplementary Figure 9: Top: displacement ellipsoid representation of **[BaH]$_2$[oxalate]·2(H$_2$O)**, ellipsoids are drawn at 50% probability. Only the major components of the disordered moieties are shown for clarity. Below: packing diagram of **[BaH]$_2$[oxalate]·2(H$_2$O)**.

[5-benzyloxytryptaminium]$_2$[sulfate]·2(H_2O)

This crystal arose in a drop obtained by mixing of 500 nl of a 1 M sodium sulfate and 500 nl of a 90% saturated 5-benzyloxytryptamine hydrochloride solution, and equilibrating against a reservoir of 1 M sodium sulfate. The achiral salt crystallized in the chiral space group $P2_1$ with two 5-benzyloxytryptaminium cations, one sulfate anion and two water molecules in the asymmetric unit. The two 5-benzyloxytryptaminium cations are protonated at the amino group. These aminium groups form multiple hydrogen bonds to two oxygen atoms of sulfate anions (N1-H11 O44(1-x,1/2+y,1-z): 2.769(3) Å; N1-H13 O45: 2.784(3) Å and N21-H211 O42 (1+x,y,z): 2.756(3) Å; N21-H213 O43(1-x,-1/2+y,1-z): 2.756 (3) Å). Finally, one indole group forms a hydrogen bond to oxygen of sulfate ion (N26-H261 O42 2.834(3) Å).

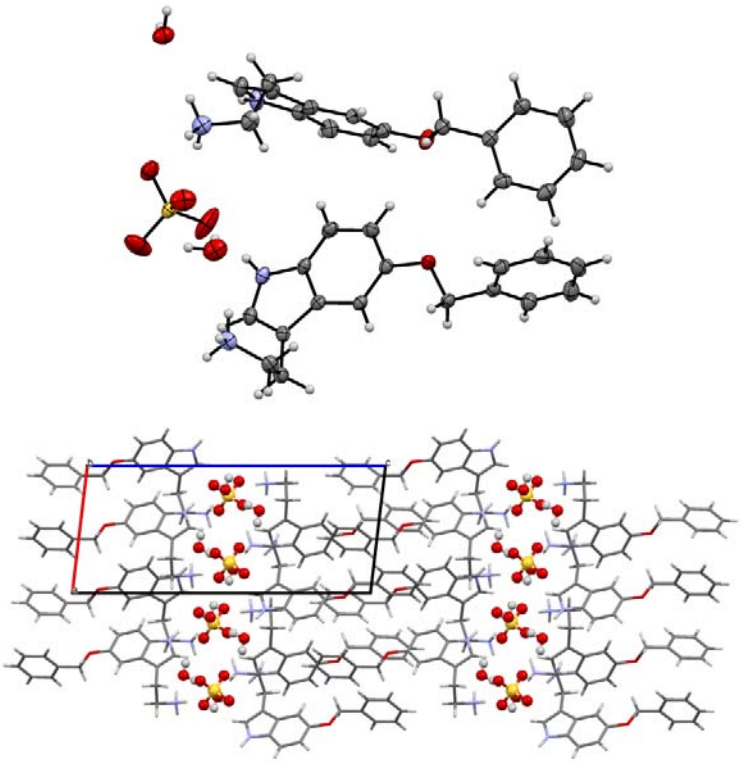

Supplementary Figure 10: Top: displacement ellipsoid representation of **[BaH]$_2$[sulfate]·2(H_2O)**, ellipsoids are drawn at 50% probability. Below: packing diagram of **[BaH]$_2$[sulfate]·2(H_2O)**.

[5-benzyloxytryptaminium][tetrafluoroborate]

The single crystal was isolated from a drop obtained by mixing 500 nl of a 4 M sodium tetrafluoroborate and 500 nl of a 90% saturated 5-benzyloxytryptamine hydrochloride solution, and equilibrating against a reservoir of 4 M sodium tetrafluoroborate. Crystals of equal quality could be obtained by taking 100 nl of both solutions instead. This complex crystallized in the monoclinic space group $P2_1/c$. The asymmetric unit consists of one 5-benzyloxytryptaminium cation, which is protonated at the amino group, and one tetrafluoroborate anion. This amino group binds to 4 fluorine atoms thus forming 2 two-centred hydrogen bonds and a combination of a three-centered hydrogen bond with a bifurcated hydrogen bond (N1-H11 F25(2-x,1-y,1-z): 2.9192(14) Å; N1-H12 F22(x,3/2-y,1/2+z): 2.8544(15) Å; N1-H12 F25: 2.9182(14) Å; N1-H13 F24(2-x,-1/2+y,3/2-z): 2.8619(14) Å).

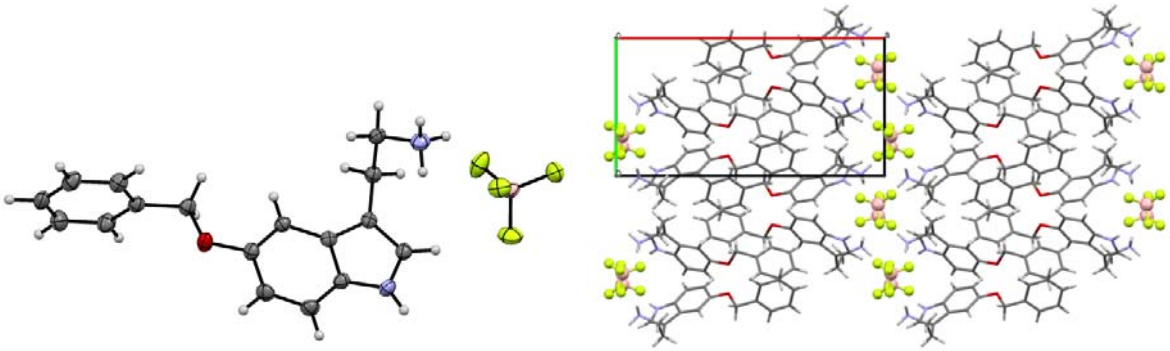

Supplementary Figure 11: Left: displacement ellipsoid representation of **[BaH][tetrafluoroborate]**, ellipsoids are drawn at 50% probability. Right: packing diagram of **[BaH][tetrafluoroborate]**.

[5-benzyloxytryptaminium][thiocyanate]

This crystal was isolated from a drop obtained by mixing 500 nl of a 3.5 M potassium thiocyanate solution and 500 nl of a 90% saturated 5-benzyloxytryptamine hydrochloride solution equilibrating against a reservoir of 3.5 M potassium thiocyanate. This complex crystallized in the monoclinic space group $P2_1/c$. The asymmetric unit consists of one 5-benzyloxytryptaminium cation, which is protonated at the amino group, and a thiocyanate anion. The amino group forms a hydrogen bond to the nitrogen atom of the thiocyanate ion (N1-H12 N21(x, y, z-1): 2.7857(19) Å).

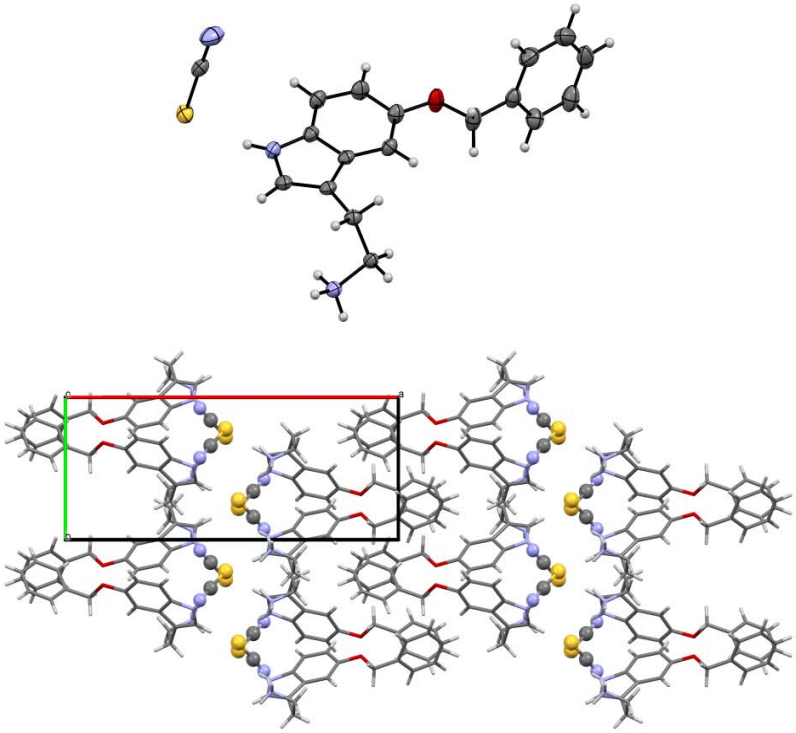

Supplementary Figure 12: Top: displacement ellipsoid representation of **[BaH][thiocyanate]**, ellipsoids are drawn at 50% probability. Below: packing diagram of **[BaH][thiocyanate]**.

The crystal structures of **[5-benzyloxytryptaminium]$_2$[succinate]** and **[5-benzyloxytryptaminium][bromide]** will be described in a later publication.

[(*R*,*S*)-carnitinenitrile][tetraphenylborate]

Crystalline material was obtained from the screening in drops containing either 200 mM sodium tetraphenylborate and 2.82 M (*R,S*)-carnitinenitrile chloride equilibrating against a reservoir of 400 mM sodium tetraphenylborate, or 100 mM sodium tetraphenylborate and 2.82 M (*R,S*)-carnitinenitrile chloride equilibrating against a reservoir of 200 mM sodium tetraphenylborate. The quality of the crystals was too low for structure determination by SCXRD. The measured crystal was obtained by recrystallization in acetone as follows: (*R,S*)-carnitinenitrile tetraphenylborate precipitated immediately after mixing a stock solution of sodium tetraphenylborate (2.82 M, 50 µl) and the stock solution of (*R,S*)-carnitinenitrile chloride (50 µl). This precipitate was filtered through a filter paper and dried on the very filter paper at room temperature. The dry powder material was dissolved in acetone till a clear solution was observed (around 100 µl acetone). The solution was evaporated at room temperature from an open vial. This complex crystallized in the monoclinic space group $P2_1/n$. The asymmetric unit consists of one carnitinenitrile cation and one tetraphenylborate anion**.** The molecule of carnitinenitrile is disordered and both enantiomers are almost in same position in a ratio of 22% *R*-enantiomer and 78% *S*-enantiomer. As the space group is centrosymmetric, no enantiomeric enrichment was observed. There is no hydrogen bonding present, as the hydroxy group of carnitinenitrile has no close acceptor.

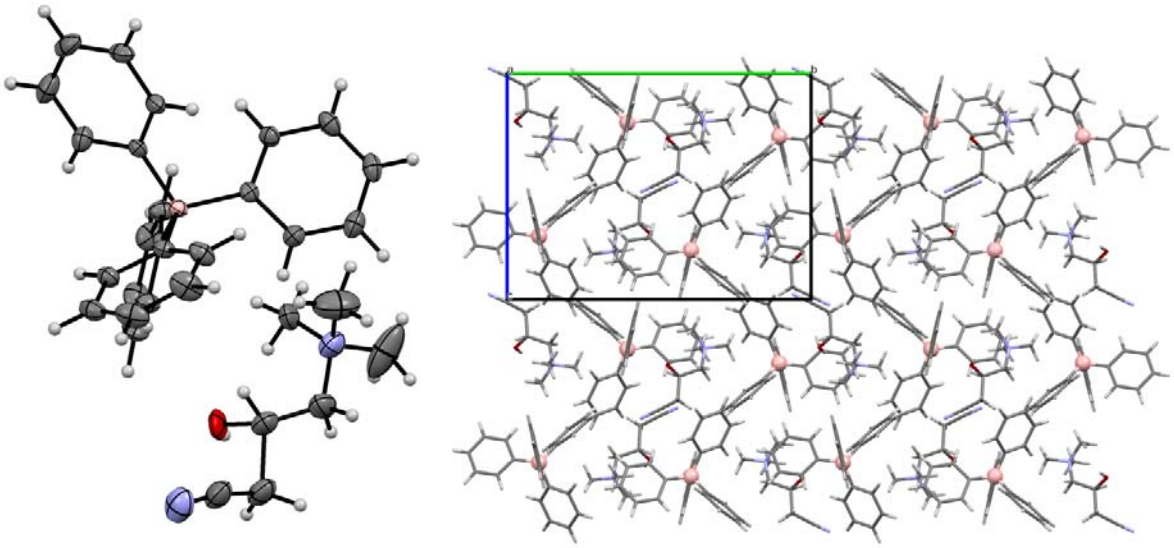

Supplementary Figure 13: Left: displacement ellipsoid representation of **[(*R*,*S*)-carnitinenitrile][tetraphenylborate]**, ellipsoids are drawn at 50% probability. Only the major conformer of the disordered hydroxy part is shown for clarity. Right: packing diagram of **[(*R*,*S*)-carnitinenitrile][tetraphenylborate]**.

[(*R*)-carnitinenitrile][tetraphenylborate]

Crystalline material was obtained from the screening in drops containing either 200 mM sodium tetraphenylborate and 2.82 M (*R*)-carnitinenitrile chloride equilibrating against a reservoir of 400 mM sodium tetraphenylborate, or 100 mM sodium tetraphenylborate and 2.82 M (*R*)-carnitinenitrile chloride equilibrating against a reservoir of 200 mM sodium tetraphenylborate. The quality of the crystals was too low for structure determination by SCXRD. The crystal used for SCXRD was crystallized on a petri dish by directly mixing two drops ethylene glycol solutions of (*R*)-carnitinenitrile chloride (10 µl, 45% of saturation) and sodium tetraphenylborate (10 µl, 25% of saturation). This mixture started to crystallize immediately and produced a good quality crystal. This complex crystallized in the orthorhombic space group $P\ 2_12_12_1$. The asymmetric unit consists of one (*R*)-carnitinenitrile cation and a tetraphenylborate anion. There is no hydrogen bond present, as the hydroxy group of carnitinenitrile has no close acceptor.

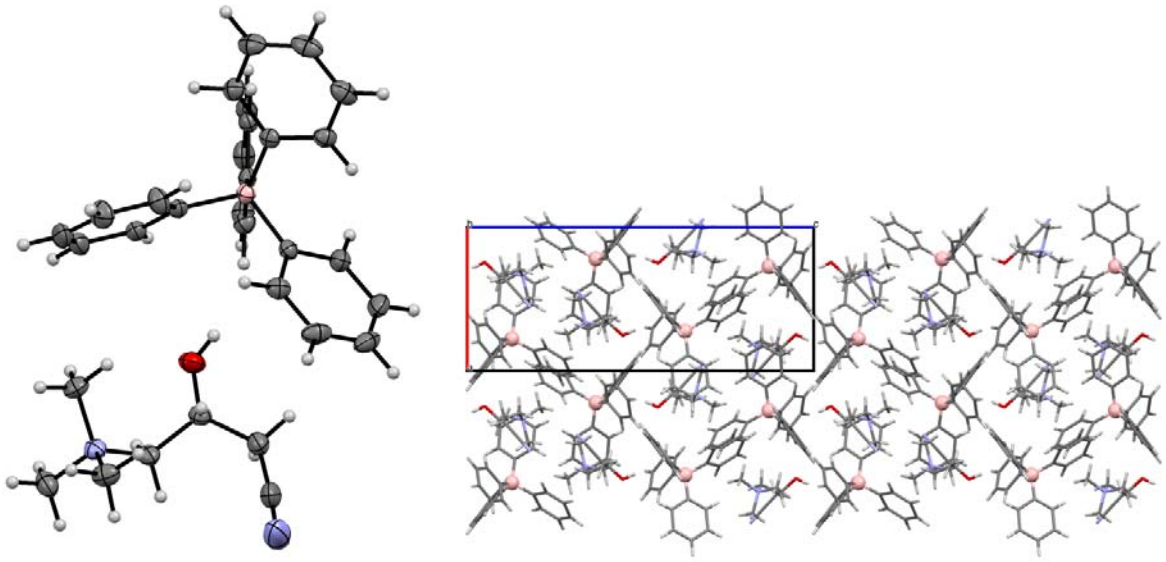

Supplementary Figure 14: Left: displacement ellipsoid representation of **[(*R*)-carnitinenitrile][tetraphenylborate]**, ellipsoids are drawn at 50% probability. Right: packing diagram of **[(*R*)-carnitinenitrile][tetraphenylborate]**.

2-(3-(3,5-bis(trifluoromethyl)phenyl)thioureido)-N,N,N-trimethylethanammonium bromide [Cat]Br

This crystal grew in a drop, which was obtained by mixing 500 nl 4 M sodium bromide and 500 nl of a 90% saturated aqueous **[Cat]I** solution, and equilibrating against a reservoir of 4 M sodium bromide. This complex crystallized in the monoclinic space group $P2_1/c$. The asymmetric unit consists of two **Cat** cations and two bromide anions. The amino groups of the thiourea form weak hydrogen bonds to the bromides (N3-H31 Br62: 3.4606(13) Å; N10-H101 Br62: 3.3343(13) Å; N33-H331 Br61: 3.4263(13) Å and N40-H401 Br61: 3.3701(14) Å). One trifluoromethyl group is disordered in each **Cat** cation.

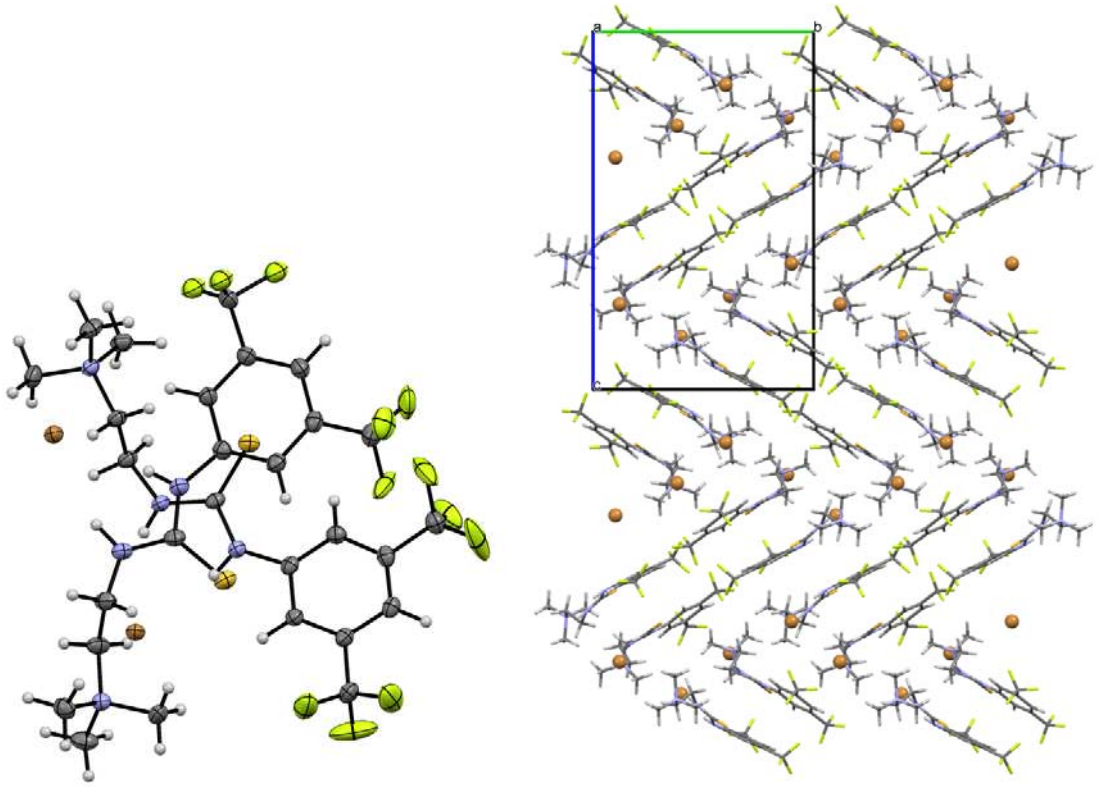

Supplementary Figure 15: Left: displacement ellipsoid representation of **[Cat][bromide]**, ellipsoids are drawn at 50% probability, for clarity only the major component of the disordered trifluoromethyl groups unit is shown. Right: packing diagram of **[Cat][bromide]**.

2-(3-(3,5-bis(trifluoromethyl)phenyl)thioureido)-N,N,N-trimethylethanammonium-potassium bis-(hexafluorophosphate) [Cat][K][PF_6]$_2$

This single crystal was directly picked from a drop obtained by mixing 500 nl 240 mM potassium hexafluorophosphate and 500 nl of a 90% saturated aqueous **[Cat]I** solution, and equilibrating against a reservoir of 240 mM potassium hexafluorophosphate. This complex crystallized in the monoclinic space group $P2_1/c$. The asymmetric unit consists of one **Cat** cation, one potassium cation and two hexafluorophosphate anions. Therefore the structure is actually a double salt. The amino groups of thiourea form hydrogen bonds with sulfur of thiourea (N3-H31 S1(x,3/2-y,-1/2+z): 3.488(2) Å and N10-H101 S1(x,3/2-y,-1/2+z): 3.398(2) Å). The potassium cation is bonded to 9 flourine atoms. Such arrangements of $K[PF_6]_4^{3-}$ have been reported previously [10-12].

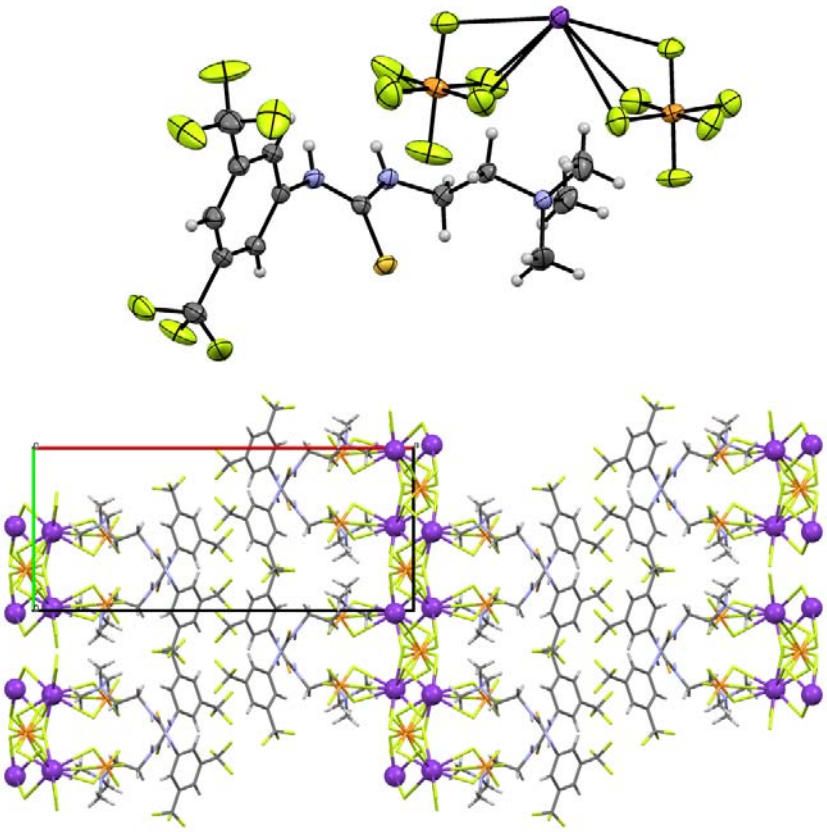

Supplementary Figure 16: Top: displacement ellipsoid representation of **[Cat][potassium][hexafluorophosphate]$_2$**, ellipsoids are drawn at 50% probability. Below: packing diagram of **[Cat][potassium][hexafluorophosphate]$_2$**.

[(1*S*,2*R*)-(+)-Ephedrinium][chloride]

This single crystal was grown in a drop obtained by mixing 100 nl of a 3.0 M sodium chloride solution and 100 nl of a 1.12 M (1*S*,2*R*)-(+)-ephedrine hydrochloride solution, and equilibrating against a reservoir of 3.0 M sodium chloride. The complex crystallized in the monoclinic, chiral space group $P2_1$. with the unit cell constants a = 7.2565(3) Å, b = 6.1232(3) Å, c = 12.5570(6) Å and β = 102.256(5)°. The structure of the other enantiomer **[(1*R*,2*S*)-(-)-ephedrinium][chloride]** (a = 7.2557(3) Å, b = 6.1228(3) Å, c = 12.5486(6) Å and β = 102.223(2)°) was previously reported [13].

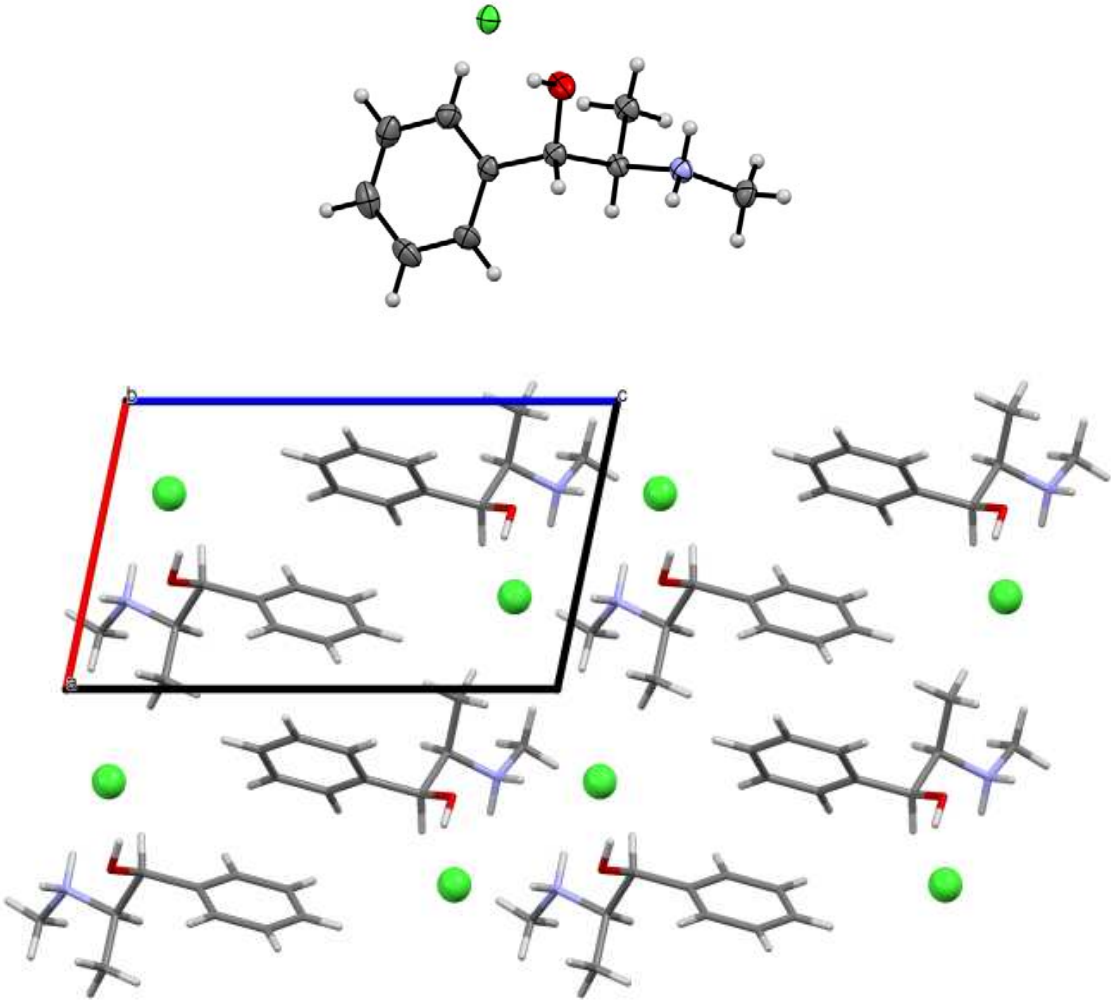

Supplementary Figure 17: Top: displacement ellipsoid representation of **[(1*S*,2*R*)-(+)-ephedrinium][chloride]**, ellipsoids are drawn at 50% probability. Below: packing diagram of **[(1*S*,2*R*)-(+)-ephedrinium][chloride]**.

[(1*S*,2*R*)-Ephedrinium][bromide]

This single crystal was grown in a drop obtained by mixing 100 nl of a 4.0 M sodium bromide solution and 100 nl of a 1.12 M (1*S*,2*R*)-(+)-ephedrine hydrochloride solution, and equilibrating against a reservoir of 3.0 M sodium bromide. The complex crystallized in the monoclinic, chiral space group $P2_1$. with the unit cell constants a = 7.4467(2) Å, b = 6.20961(16) Å, c = 12.5863(4) Å and β = 101.176(3)°. The cell constants of the opposite enantiomer **[(1*R*,2*S*)-ephedrinium][bromide]** at room temperature were previously reported as follows: a = 12.74 Å, b = 6.20 Å, c = 7.62 Å and β = 100.80° [14]. The structure is isostructural compared with the chloride salt (see the previous structure and ref. [13]).

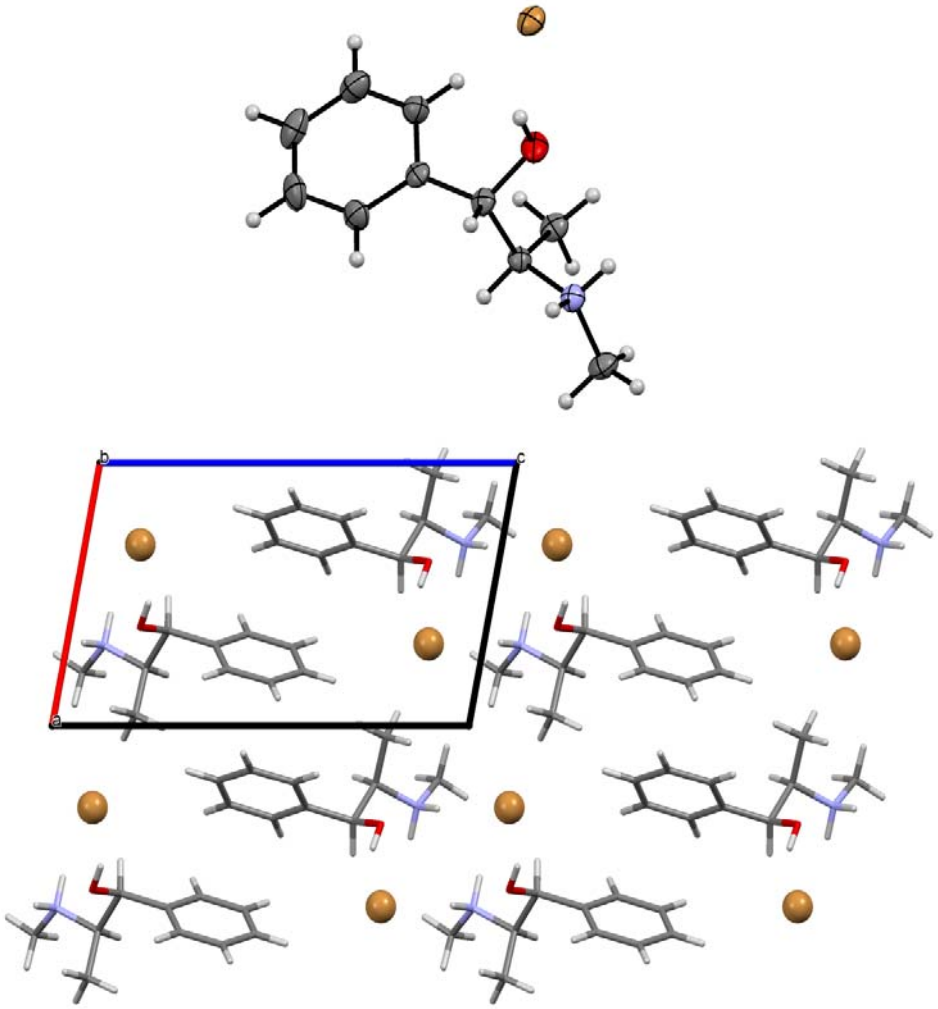

Supplementary Figure 18: Top: displacement ellipsoid representation of **[(1*S*,2*R*)-ephedrinium][bromide]**, ellipsoids are drawn at 50% probability. Below: packing diagram of **[(1*S*,2*R*)-ephedrinium][bromide]**.

[(1*S*,2*R*)-Ephedrinium][iodide], polymorph II

Crystals were obtained in a drop containing 2.67 M sodium iodide and 0.31 M (1*S*,2*R*)-(+)-ephedrine hydrochloride that was equilibrated by vapour diffusion against a reservoir of 5.34 M sodium iodide at 4°C. The complex crystallized in the monoclinic, chiral space group $P2_1$. with the unit cell constants a = 5.40542(18) Å, b = 6.94898(18) Å, c = 16.0701(4) Å and β = 95.864(3)°. This new crystal form is a polymorph of the previously reported orthorhombic form of the opposite enantiomer **[(1*R*,2*S*)-ephedrinium][iodide]** (a = 25.66 Å, b = 7.33 Å, c = 19.14 Å), which was published in 1933 [14]. This orthorhombic crystal form was originally prepared in 1909 by evaporation of an ethanolic solution of [(1*R*,2*S*)-ephedrinium][iodide] [15].

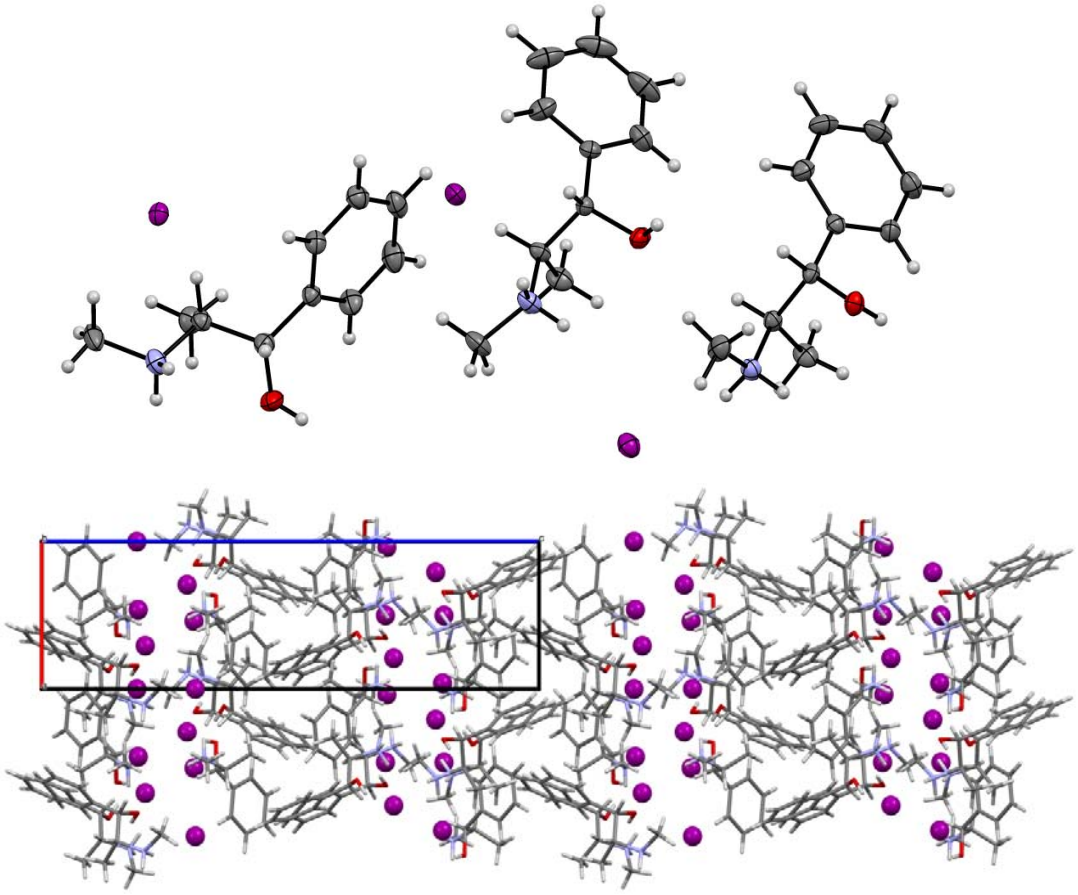

Supplementary Figure 19: Top: displacement ellipsoid representation of **[(1*S*,2*R*)-ephedrinium][iodide]**, polymorph II, ellipsoids are drawn at 50% probability. Below: packing diagram of **[(1*S*,2*R*)-ephedrinium][iodide]**, polymorph II.

[(1*S*,2*R*)-Ephedrinium][iodide], polymorph I

Crystals of polymorph I were obtained by mixing 1 ml of a 0.62 M solution of (1*S*,2*R*)-(+)-ephedrine hydrochloride and 1 ml of a 5.34 M solution of sodium iodide. Large crystals grew overnight (Supplementary Fig. 20). A suitable single crystal was chosen for the X-ray diffraction experiment. The unit cell was essentially equal to that found for the opposite enantiomer, which had already been reported in 1933 (see also the previous discussion of the other polymorph) [14]. The complex crystallized in the orthorhombic, chiral space group $P2_12_12_1$ and contained three molecules in the asymmetric unit.

Supplementary Figure 20: Microscope picture of crystals grown in a 15 ml polypropylene centrifuge tube by mixing 1 ml of a 0.62 M solution of (1*S*,2*R*)-(+)-ephedrine hydrochloride and 1 ml of a 5.34 M solution of sodium iodide. The scale bar corresponds to 1 mm.

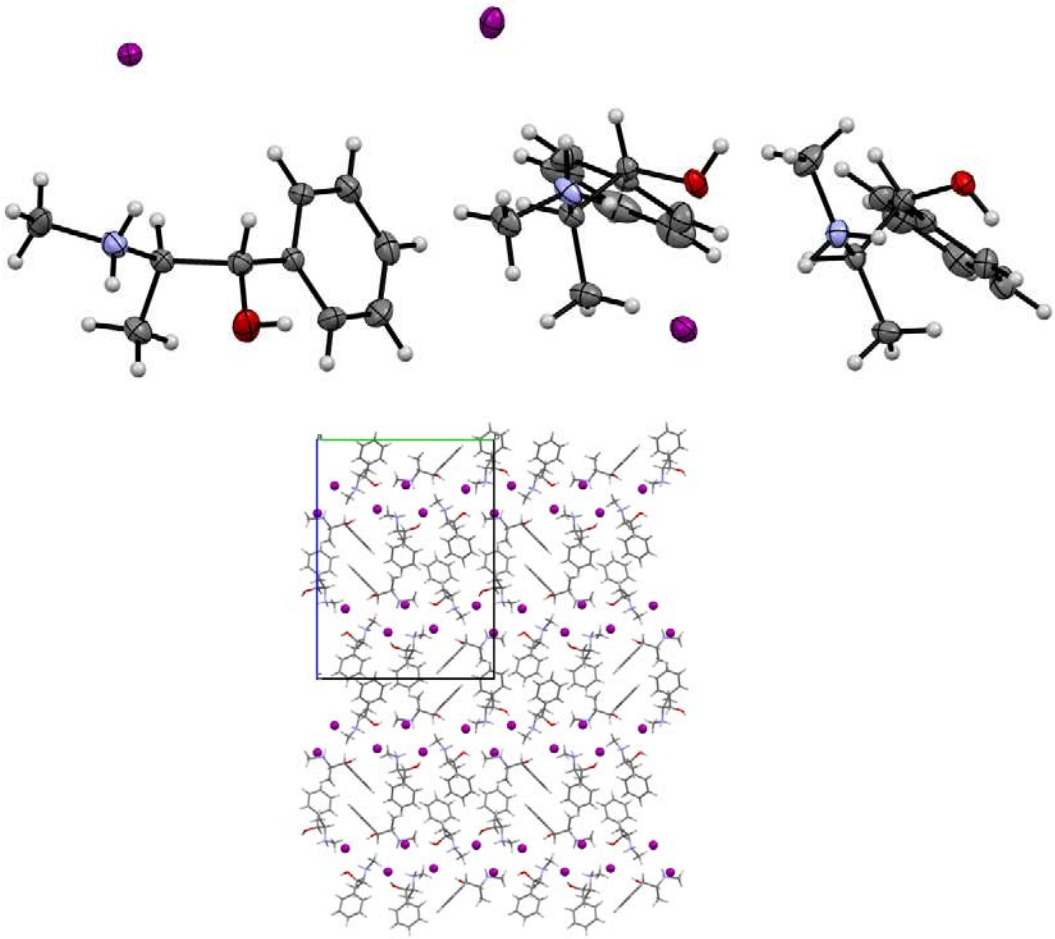

Supplementary Figure 21: Top: displacement ellipsoid representation of the asymmetric unit of **[(1*S*,2*R*)-ephedrinium][iodide]**, polymorph I, ellipsoids are drawn at 50% probability. Below: packing diagram of **[(1*S*,2*R*)-ephedrinium][iodide]**, polymorph I.

[(1*S*,2*R*)-Ephedrinium]$_2$[oxalate]

Crystals were obtained from a drop containing 0.069 M disodium oxalate and 0.155 M (1*S*,2*R*)-(+)-ephedrine hydrochloride that was equilibrated by vapour diffusion against a reservoir of 0.138 M disodium oxalate. The crystals were of sufficient size and excellent quality that they could even be measured with the relatively weak molybdenum X-ray radiation. The complex crystallized in the monoclinic, chiral space group *C*2. The asymmetric unit contains one protonated ephedrine cation and one half an of oxalate anion. Because of the used X-ray wavelength and the presence of exclusively light elements, the Flack x and the Parson's z parameters calculated by *Platon* [16] were unreliable (0.2(2) and 0.15(19) respectively), however using the Hooft method [17] and assuming no racemic twinning gave a very low probability *p*2(wrong) of $1.2 \cdot 10^{-4}$ that the model assumes the wrong enantiomer. As the program *Platon* only calculates *p*2(right), *p*2(wrong) was calculated with the formula given at http://www.absolutestructure.com/faq: *p*2(wrong) = [*p*3(wrong)/(*p*3(wrong) + *p*3(right))]). The protonated secondary amine forms two hydrogen bonds (N1-H11 O11: 2.7536(14) Å and N1-H12 O11(-x+1/2,y-1/2,-z+1): 2.8233(14) Å) and the alcohol one hydrogen bond (O1-H1A O1(-x,y-1,-z+1): 2.6730(13) Å).

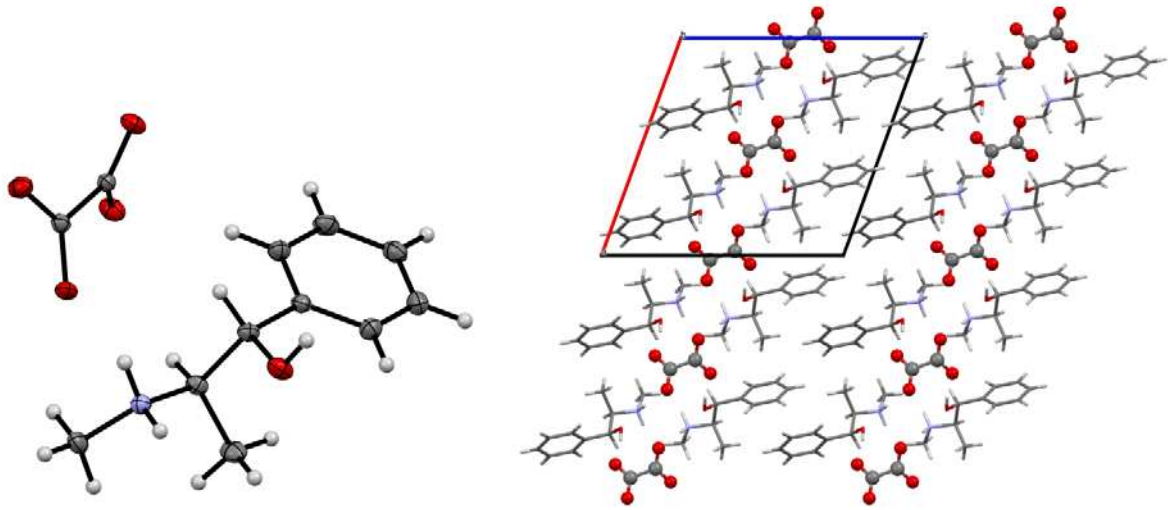

Supplementary Figure 22: Left: displacement ellipsoid representation of **[(1*S*,2*R*)-ephedrinium]$_2$[oxalate]**, ellipsoids are drawn at 50% probability. One protonated ephedrine cation and a whole oxalate anion are shown. Right: packing diagram of **[(1*S*,2*R*)-ephedrinium]$_2$[oxalate]**.

[(1*S*,2*R*)-Ephedrinium][thiocyanate]

This single crystal was directly picked from a drop obtained by mixing 100 nl of a 1.75 M potassium thiocyanate solution and 100 nl of a 1.12 M (1*S*,2*R*)-(+)-ephedrine hydrochloride solution, and equilibrating against a reservoir of 1.75 M potassium thiocyanate. The complex crystallized in the orthorhombic, chiral space group $P2_12_12_1$. with the unit cell constants a = 6.09862(6) Å, b = 7.52704(9) Å and c = 27.3811(3)Å.

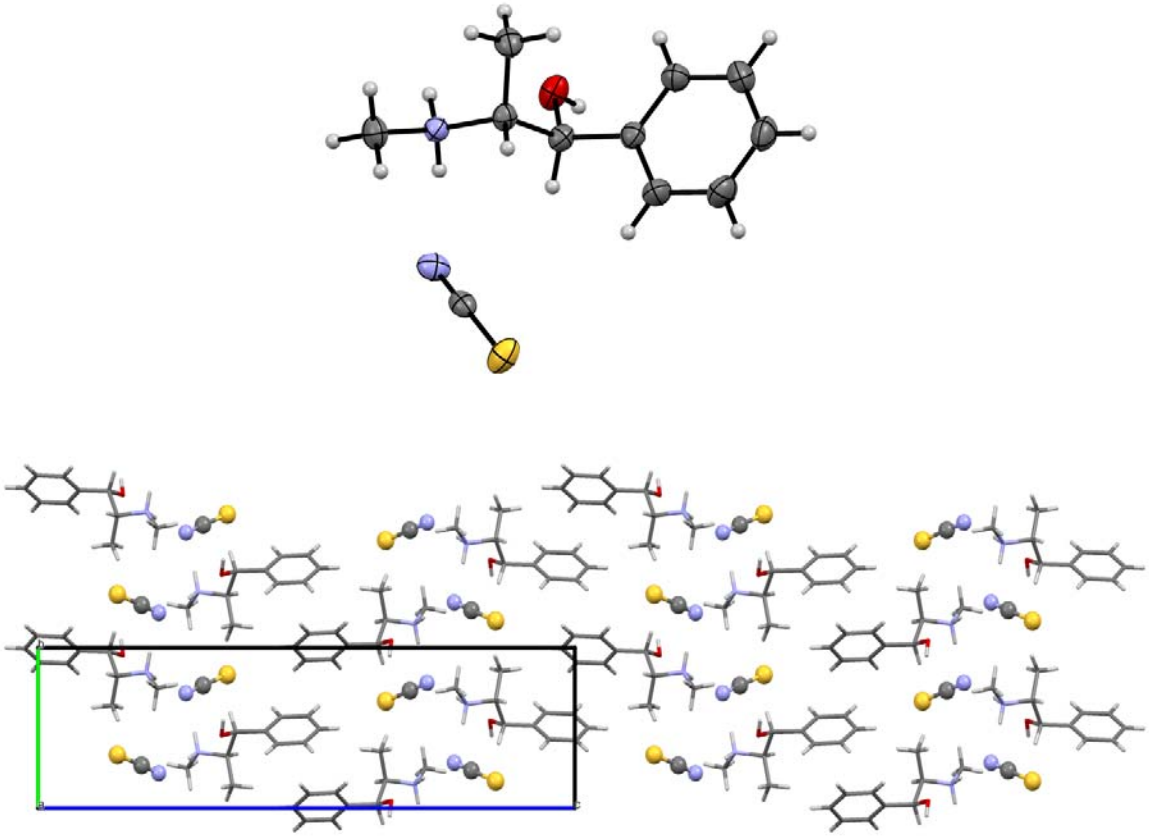

Supplementary Figure 23: Top: displacement ellipsoid representation of **[(1*S*,2*R*)-ephedrinium][thiocyanate]**, ellipsoids are drawn at 50% probability. Below: packing diagram of **[(1*S*,2*R*)-ephedrinium][thiocyanate]**.

[Trazodonium][iodide]

Crystals of the iodide salt were grown in a drop obtained by mixing 500 nl 5.34 M NaI and 500 nl of a 90% saturated aqueous trazodone hydrochloride solution, and equilibrating against a reservoir of 5.34 M NaI. The asymmetric unit contains one protonated trazodone cation and an iodide anion. The trazodone cation is monoprotonated at the piperazine amine atom that is connected solely to aliphatic carbon atoms. This ammonium group forms a weak hydrogen bond to the iodide anion (N14-H14A I31: 3.6541(15) Å).

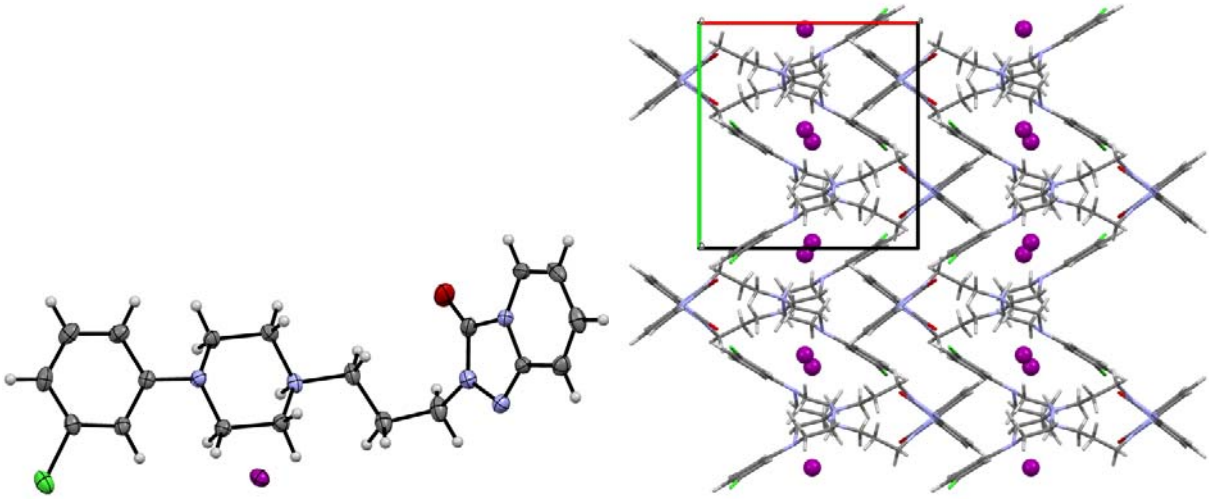

Supplementary Figure 24: Left: displacement ellipsoid representation of **[trazodonium][iodide]**, ellipsoids are drawn at 50% probability. Right: packing diagram of **[trazodonium][iodide]**.

[Trazodonium]$_2$[oxalate]·10(H_2O)

This crystal was obtained at 4°C from a drop containing 69 mM Na_2oxalate and 12 mM trazadone hydrochloride equilibrating against a reservoir of 138 mM Na_2oxalate. This complex crystallized in the monoclinic space group *I*2/a. The asymmetric unit consists of one trazodonium cation, half an oxalate dianion and 6 sites for water molecules, of which 2 are half occupied. The trazodone cation is monoprotonated at the piperazine amine atom that is connected solely to aliphatic carbon atoms. This ammonium unit forms a double bifurcated hydrogen bond to the oxalate anion (N14-H14A O28: 2.7510(17) Å and N14-H14A O29(-x+1, -y+1, -z+1): 2.9474(17) Å respectively). The oxalate anion sits on an inversion center, it is sandwiched between two ammonium units of the trazodone.

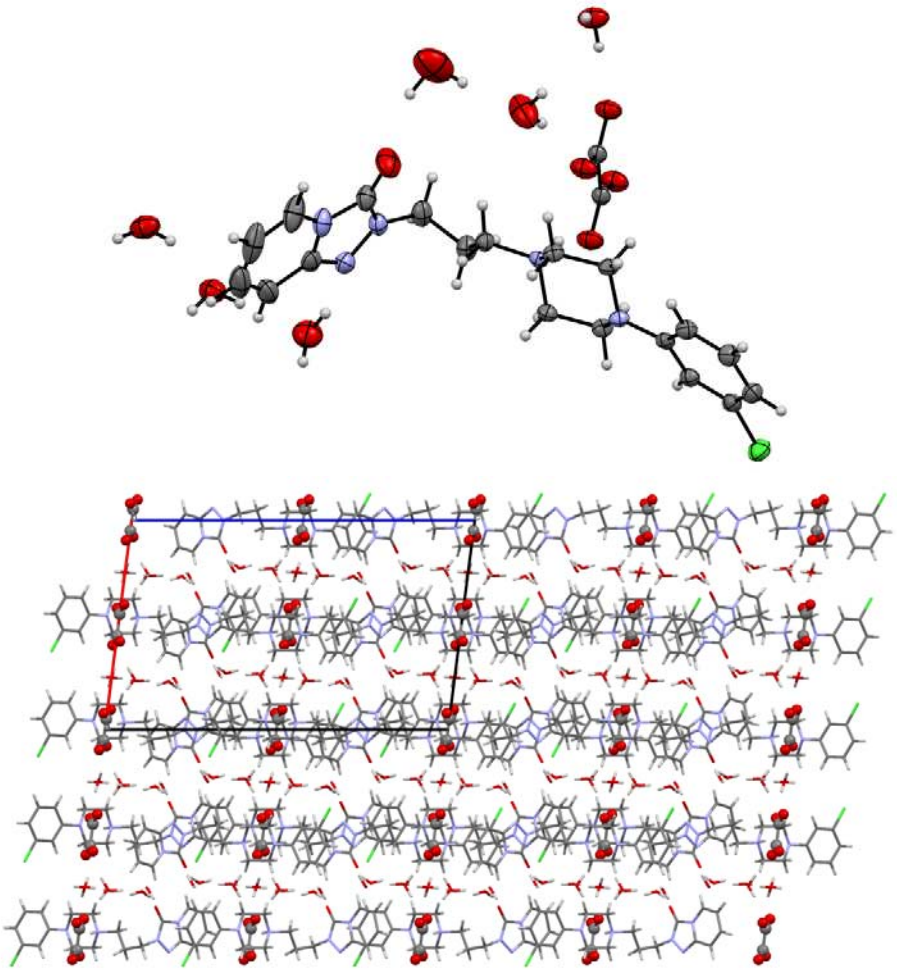

Supplementary Figure 25: Top: displacement ellipsoid representation of **[trazodonium]$_2$[oxalate]·10(H_2O)**, ellipsoids are drawn at 50% probability. One molecule of a protonated trazodone and a whole oxalate molecule is shown (see also paragraph above for a further discussion of the content of the asymmetric unit). Below: packing diagram of **[trazodonium]$_2$[oxalate]·10(H_2O)]**.

Trazodone·2(H_2O)

This crystal was obtained from a solution containing 141 mM disodium-(DL)-tartrate and 23.5 mM trazodone that was equilibrated by vapour diffusion against a reservoir of 242 mM disodium-(DL)-tartrate. After covering the drop with oil (Infineum V8512, formerly known as Paratone N), crystals started to form at the interface between the oil and the aqueous phase and grew into the oil. The asymmetric unit contains one neutral trazodone molecule and two water molecules, one is disordered over 2 positions (ratio 1:1), the other is disordered over 3 positions (ratio 5:4:1). In addition, the triazolo-pyridinone ring is disordered in a 9:1 ratio.

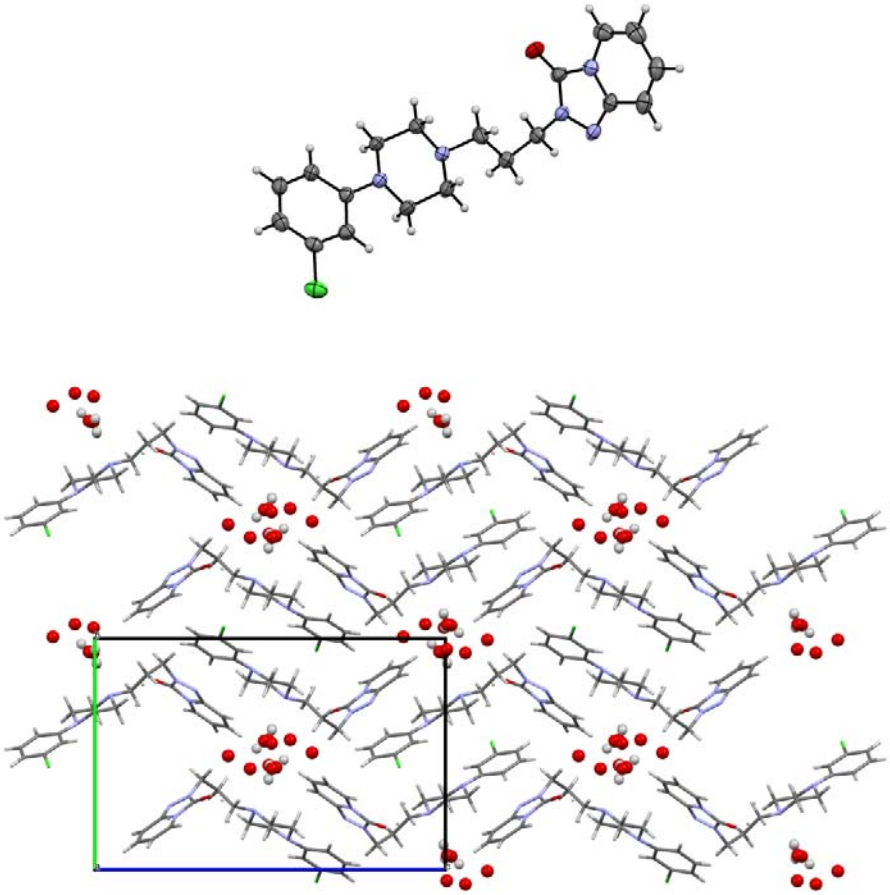

Supplementary Figure 26: Top: displacement ellipsoid representation of **trazodone·2(H_2O)**, ellipsoids are drawn at 50% probability. For clarity, the disordered minor component of the trazodone molecules and the disordered water molecules are omitted. Below: packing diagram of **trazodone·2(H_2O)**.

Supplementary Table 2. Composition and concentration of the counterion salts in the 96 wells of the organic cation crystallization screen.

Well number	**Chemical name**	**Conc. [M]**
1	Sodium chloride	3.00
2	Sodium chloride	1.50
3	Sodium bromide	4.00
4	Sodium bromide	2.00
5	Sodium iodide	5.30
6	Sodium iodide	2.50
7	Sodium iodide	1.25
8	Potassium thiocyanate	7.30
9	Potassium thiocyanate	3.50
10	Potassium thiocyanate	1.75
11	Sodium dicyanamide	0.70
12	Sodium tetrafluoroborate	4.00
13	Sodium tetrafluoroborate	2.00
14	Potassium hexafluorophosphate	0.24
15	Sodium tetraphenylborate	0.40
16	Sodium tetraphenylborate	0.20
17	Disodium sulfate	1.00
18	Sodium methanesulfonate	3.60
19	Sodium methanesulfonate	1.80
20	Sodium triflate	0.80
21	Sodium isethionate	2.20
22	Sodium isethionate	1.10
23	Sodium (+/-)-camphorsulfonate	2.28
24	Sodium benzenesulfonate	0.98
25	Sodium 3-nitrobenzensulfonate	0.42
26	Sodium *p*-toluenesulfonate	0.15
27	Sodium 1-naphthalensulfonate	0.35
28	Sodium 2-naphthalensulfonate	0.13
29	Disodium 2,6-naphthalenedisulfonate	0.085
30	Sodium nitrate	4.60
31	Sodium nitrate	2.30

32	Sodium benzoate	1.80
33	Sodium salicylate	2.20
34	Sodium salicylate	1.10
35	Sodium 4-aminosalicylate dihydrate	1.50
36	Sodium meta-hydroxybenzoate	1.30
37	Sodium nicotinate	2.96
38	Sodium nicotinate	1.48
39	Potassium hydrogen phthalate	0.27
40	Disodium isophthalate	1.40
41	Disodium terephthalate	0.060
42	Disodium pamoate	0.050
43	Sodium formate	6.00
44	Sodium formate	3.00
45	Sodium acetate	2.60
46	Sodium trifluoroacetate	2.40
47	Sodium 2-phenylpropionate	1.70
48	Sodium DL-mandelate	0.25
49	Sodium D-mandelate	0.25
50	Sodium L-mandelate	0.25
51	Sodium 1-naphthalenacetate	0.43
52	Sodium diphenylacetate	0.33
53	Sodium *N*-acetylglycinate	2.28
54	Sodium hippurate	1.46
55	Sodium pyrrolidone carboxylate	4.96
56	Sodium propionate	5.20
57	Sodium propionate	2.60
58	Sodium DL-lactate	3.42
59	Sodium L-lactate	3.42
60	Sodium pyruvate	3.00
61	Sodium pyruvate	1.50
62	Sodium valerate	3.19
63	Sodium hexanoate	2.70
64	Sodium 2-ethylhexanoate	4.20
65	Sodium 2-ethylhexanoate	2.10

66	Potassium gluconate	1.10
67	Sodium octanoate	1.56
68	Sodium hydrogen carbonate	0.60
69	Disodium carbonate	1.00
70	Disodium oxalate	0.14
71	Disodium malonate	2.97
72	Disodium succinate	1.13
73	Disodium maleate	0.66
74	Disodium fumarate	0.73
75	Disodium DL-malate	2.27
76	Disodium L-malate	2.92
77	Sodium potassium L-tartrate	1.40
78	Disodium DL -tartrate	0.55
79	Disodium L-tartrate	1.00
80	Disodium (+)-O,O'-dibenzoyl-D-tartrate	0.26
81	Potassium antimony tartrate	0.054
82	Disodium N-acetylglutamate	1.63
83	Disodium adipate	1.19
84	Potassium D-saccharate	0.050
85	Trisodium citrate dihydrate	0.90
86	Sodium DL-aspartate	0.25
87	Sodium L-aspartate	0.25
88	Sodium L-glutamate	2.00
89	Sodium L-glutamate	1.00
90	Sodium diethyldithiocarbamate	0.011
91	Sodium saccharine	1.57
92	Disodium hydrogen phosphate	0.43
93	Sodium dihydrogen phosphate	4.00
94	Sodium dihydrogen phosphate	2.00
95	Disodium citrate	0.93
96	Trisodium phosphate (dodecahydrate)	0.36

Supplementary Table 3: Crystallographic data of the chloride, iodide, dihydrogenphosphate and antimony-L-tartrate salts of 5-benzyloxytryptaminium.

name	**[BaH][chloride]**	**[BaH][iodide]**	**[BaH][dihydrogen phosphate]**	**$[BaH]_2$ [antimony L-tartrate]**·2(H_2O)
Empirical formula	$[C_{17}H_{19}N_2O]Cl$	$[C_{17}H_{19}N_2O]I$	$[C_{17}H_{19}N_2O]$ $[H_2O_4P]$	$[C_{17}H_{19}N_2O]_2$ $[C_8H_4O_{12}Sb_2]$ ·2(H_2O)
Diffractometer	Synergy	Synergy	Synergy	Synergy
Wavelength (Å)	1.54180	1.54180	1.54180	1.54180
mol. weight (g/mol)	302.80	394.26	364.34	1106.34
Crystal system	monoclinic	monoclinic	monoclinic	monoclinic
Space group	$P2_1/c$	$P2_1/c$	$P2_1/c$	$C2$
a (Å)	18.7661(5)	19.6674(3)	20.7561(2)	22.3684(7)
b (Å)	8.8339(2)	8.1224(1)	9.5134(1)	8.4156(1)
c (Å)	9.6084(3)	10.8447(2)	8.5352(1)	15.6852(4)
α (°)	90	90	90	90
β (°)	100.318(3)	105.2892(16)	96.5078(9)	130.585(5)
γ (°)	90	90	90	90
Volume ($Å^3$)	1567.10(7)	1671.09(5)	1674.51(3)	2242.36(19)
Z	4	4	4	2
Density(calc.) (g/cm^3)	1.283	1.567	1.445	1.639
Linear abs. coeff. (mm^{-1})	2.152	15.054	1.741	10.200
F(000)	640.0	784.0	768.0	1112.0
Crystal size (mm^3)	0.26 × 0.15 × 0.02	0.56 × 0.44 × 0.02	0.23 × 0.15 × 0.01	0.39 × 0.03 × 0.01
Crystal description	plate, colorless	plate, colorless	plate, colorless	lath, colorless
θ range (°)	4.790; 74.494	4.662; 74.462	4.288; 75.865	3.711; 78.973
Reflections collected	30743	33730	34497	22761
Indep. reflections	3187 [R_{int} = 0.0435]	3418 [R_{int} = 0.0527]	3487 [R_{int} = 0.0301]	4676 [R_{int} = 0.0948]
Reflections obs.	2941	3145	3276	4563
Criterion for obs.	I > 2.0σ(I)	I > 2.0σ(I)	I > 2.0σ(I)	I > 2.0σ(I)
Completeness to θ (°)	0.999 to 74.494	1 to 74.462	0.999 to 75.865	0.998 to 77.394
Absorption corr.	multi-scan	multi-scan	multi-scan	multi-scan
Min. and max. transm.	0.74 and 0.96	0.02 and 0.73	0.44 and 0.98	0.25 and 0.89
Reflections / restraints / parameters	3187 / 0 / 190	3418 / 0 / 190	3487 / 0 / 226	4676 / 5 / 290
Goodness-of-fit on F^2	0.9683	0.9797	0.9648	0.9417
Final R indices [I > 2.0σ(I)]	R_1 = 0.0381 wR2 = 0.0949	R_1 = 0.0226 wR2 = 0.0605	R_1 = 0.0294 wR2 = 0.0750	R_1 = 0.0453 wR2 = 0.1189
R indices (all data)	R_1 = 0.0406 wR_2 = 0.0965	R_1 = 0.0246 wR_2 = 0.0622	R_1 = 0.0312 wR_2 = 0.0761	R_1 = 0.0458 wR_2 = 0.1194
Final $\Delta\rho_{max,min}$ ($e^-/Å^3$)	0.42 and −0.37	1.01 and −0.50	0.25 and −0.38	2.37 and −0.68
Flack parameter	not applicable	not applicable	not applicable	-0.010(9)
CSD number	1585748	1585750	1585749	1585752

Supplementary Table 4: Crystallographic data of the L-tartrate, oxalate, sulfate, tetrafluoroborate and thiocyanate salts of 5-benzyloxytryptaminium.

name	**$[BaH]_2$ [L-tartarate]** $\cdot 3.35(H_2O)$	**$[BaH]_2$[oxalate]** $\cdot 2(H_2O)$	**$[BaH]_2$[sulfate]** $\cdot 2\ (H_2O)$	**[BaH] [tetrafluoro-borate]**	**[BaH] [thiocyanate]**
Empirical formula	$[C_{17}H_{19}N_2O]_2$ $[C_4H_4O_6]$ $\cdot 3.35(H_2O)$	$[C_{17}H_{19}N_2O]_2$ $[C_2O_4]\cdot 2(H_2O)$	$[C_{17}H_{19}N_2O]$ $[O_4S]\cdot 2(H_2O)$	$[C_{17}H_{19}N_2O]$ $[BF_4]$	$[C_{17}H_{19}N_2O]$ [NCS]
Diffractometer	Synergy	Synergy	Synergy	Synergy	Synergy
Wavelength (Å)	1.54180	1.54180	1.54180	1.54180	1.54180
mol. weight (g/mol)	742.37	654.72	666.80	354.15	325.43
Crystal system	monoclinic	monoclinic	monoclinic	monoclinic	monoclinic
Space group	$P2_1$	$P2_1$	$P2_1$	$P2_1/c$	$P2_1/c$
a (Å)	8.8100(1)	9.0081 (1)	8.6454 (1)	19.5805 (2)	19.8981 (7)
b (Å)	9.7133(2)	9.3218 (1)	9.4630 (1)	9.7595 (1)	8.0213 (2)
c (Å)	21.7147(4)	19.4957 (2)	20.0392 (2)	8.9644 (1)	10.8806 (3)
α (°)	90	90	90	90	90
β (°)	100.1689(16)	95.3510 (9)	96.7530 (9)	103.1581 (12)	100.435 (3)
γ (°)	90	90	90	90	90
Volume ($Å^3$)	1829.03(6)	1629.95 (3)	1628.06 (3)	1668.08 (3)	1707.92 (9)
Z	2	2	2	4	4
Density(calc.) (g/cm^3)	1.349	1.334	1.360	1.410	1.266
Linear abs. coeff. (mm^{-1})	0.83	0.783	1.373	1.013	1.739
F(000)	789.6	692.0	708.0	736.0	688.0
Crystal size (mm^3)	0.08 × 0.06 × 0.007	0.11 × 0.10 × 0.02	0.08 × 0.05 × 0.03	0.26 × 0.24 × 0.01	0.12 × 0.07 × 0.02
Crystal description	plate, colorless	plate, colorless	plate, colorless	plate, colorless	plate, colorless
θ range (°)	4.137; 74.489	4.556; 74.493	4.444; 74.500	4.638; 74.504	4.519; 74.390
Reflections collected	31303	34550	34569	18232	10335
Indep. reflections	7406 [R_{int} = 0.0442]	6622 [R_{int} = 0.0325]	6613 [R_{int} = 0.0414]	3411 [R_{int} = 0.0336]	3450 [R_{int} = 0.0220]
Reflections obs.	6788	6365	6209	3088	2987
Criterion for obs.	I > 2.0σ(I)	I > 2.0σ(I)	I > 2.0σ(I)	I > 2.0σ(I)	I > 2.0σ(I)
Completeness to θ (°)	0.999 to 67.680	0.997 to 74.493	0.999 to 74.500	1.000 to 74.504	0.995 to 74.390
Absorption corr.	gaussian	multi-scan	multi-scan	multi-scan	multi-scan
Min. and max. transm.	0.803 and 1	0.67 and 0.98	0.81 and 0.97	0.21 and 0.99	0.83 and 0.97
Reflections / restraints /	7406 / 21 / 526	6622 / 67 / 516	6613 / 5 / 425	3411 / 0 / 226	3450 / 0 / 208

parameters					
Goodness-of-fit on F^2	1.049	0.9838	0.9540	0.9896	0.9770
Final R ind. [$I > 2.0\sigma(I)$]	$R_1 = 0.0411$ $wR_2 = 0.1118$	$R_1 = 0.0344$ $wR_2 = 0.0973$	$R_1 = 0.0417$ $wR_2 = 0.1038$	$R_1 = 0.0361$ $wR_2 = 0.0942$	$R_1 = 0.0338$ $wR_2 = 0.0819$
R indices (all data)	$R_1 = 0.0451$ $wR_2 = 0.1144$	$R_1 = 0.0356$ $wR_2 = 0.0984$	$R_1 = 0.0441$ $wR_2 = 0.1063$	$R_1 = 0.0399$ $wR_2 = 0.0971$	$R_1 = 0.0401$ $wR_2 = 0.0873$
Final $\Delta\rho_{max,min}$ ($e^-/Å^3$)	0.51 and -0.37	0.31 and −0.24	0.80 and −0.39	0.28 and −0.21	0.38 and −0.26
Flack parameter	-0.11(8)	0.17(14)	0.114(15)	not applicable	not applicable
CSD number	1585755	1585751	1585754	1585747	1585753

Supplementary Table 5: Summary of crystals containing carnitinenitrile

name	**[(+/-)-Car][tetraphenylborate]**	**[(-)-Car][tetraphenylborate]**
Empirical formula	$[C_7H_{15}N_2O][C_{24}H_{20}B]$	$[C_7H_{15}N_2O][C_{24}H_{20}B]$
Diffractometer	Xcalibur	SuperNova
Wavelength (Å)	0.71073	1.5418
mol. weight (g/mol)	462.44	462.44
Crystal system	monoclinic	orthorhombic
Space group	$P2_1/n$	$P2_12_12_1$
a (Å)	10.1433 (4)	9.49835 (14)
b (Å)	18.6189 (6)	11.89113 (17)
c (Å)	14.0467 (5)	22.8675 (3)
α (°)	90	90
β (°)	99.569 (3)	90
γ (°)	90	90
Volume ($Å^3$)	2615.91 (16)	2582.79 (6)
Z	4	4
Density(calc.) (g/cm^3)	1.174	1.189
Linear abs. coeff. (mm^{-1})	0.070	0.542
F(000)	992.0	992.0
Crystal size (mm^3)	0.48 × 0.46 × 0.05	0.43 × 0.10 × 0.09
Crystal description	plate, colorless	prism, colorless
θ range (°)	2.311; 30.505	3.866; 74.454
Reflections collected	33386	21298
Indep. reflections	7988 [R_{int} = 0.0359]	5254 [R_{int} = 0.0260]
Reflections obs.	6470	5101
Criterion for obs.	I > 2.0σ(I)	I > 2.0σ(I)
Completeness to θ (°)	1.000 to 30.505	1.000 to 74.454
Absorption corr	multi-scan	multi-scan
Min. and max. transm.	0.99 and 1.00	0.69 and 0.95
Reflections / restraints / parameters	7983 / 128 / 407	5254 / 0 / 316
Goodness-of-fit on F^2	1.0133	0.9920
Final R ind. [I > 2.0σ(I)]	R_1 = 0.0578, wR_2 = 0.1365	R_1 = 0.0272, wR_2 = 0.0703
R indices (all data)	R_1 = 0.0721, wR_2 = 0.1480	R_1 = 0.0281, wR_2 = 0.0713
Final $\Delta\rho_{max,min}$ ($e^-/Å^3$)	0.47 and −0.46	0.21 and −0.11
Flack parameter	not applicable	0.0(3)
CSD number	1585762	1585761

Supplementary Table 6: Crystallographic summary of the crystals containing 2-(3-(3,5-bis(trifluoromethyl)phenyl)-thioureido)-N,N,N-trimethylethanammonium (**Cat**)

name	**[Cat][bromide]**	**[Cat][potassium][hexafluorophosphate]$_2$**
Empirical formula	$[C_{14}H_{18}F_6N_3S]Br$	$[C_{14}H_{18}F_6N_3S]K[F_6P]_2$
Diffractometer	Synergy	Synergy
Wavelength (Å)	1.54180	1.54180
mol. weight (g/mol)	454.27	703.39
Crystal system	monoclinic	monoclinic
Space group	$P2_1/c$	$P2_1/c$
a (Å)	10.9874 (1)	24.3732 (2)
b (Å)	14.2737 (1)	10.4084 (1)
c (Å)	23.2106 (1)	9.9932 (1)
α (°)	90	90
β (°)	90.2783 (5)	93.1701 (9)
γ (°)	90	90
Volume (Å^3)	3640.10 (4)	2531.26 (4)
Z	8	4
Density(calc.) (g/cm^3)	1.658	1.846
Linear abs. coeff. (mm^{-1})	4.736	5.196
F(000)	1824.0	1400.0
Crystal size (mm^3)	0.48 × 0.13 × 0.06	0.11 × 0.05 × 0.02
Crystal description	lath, colorless	lath, colorless
θ range (°)	3.635; 72.121	3.632; 74.496
Reflections collected	46471	49106
Indep. reflections	7149 [R_{int} = 0.0269]	5098 [R_{int} = 0.0450]
Reflections obs.	6871	4507
Criterion for obs.	I > 2.0σ(I)	I > 2.0σ(I)
Completeness to θ (°)	0.995 to 72.121	0.987 to 74.33
Absorption corr.	multi-scan	multi-scan
Min. and max. transm.	0.11 and 0.76	0.64 and 0.92
Reflections / restraints / parameters	7149 / 22 / 535	5098 / 79 / 408
Goodness-of-fit on F^2	1.0022	1.0134
Final R ind. [I > 2.0σ(I)]	R_1 = 0.0221, wR_2 = 0.0551	R_1 = 0.0441, wR_2 = 0.1053
R indices (all data)	R_1 = 0.0230, wR_2 = 0.0556	R_1 = 0.0496, wR_2 = 0.1087
Final $\Delta\rho_{max,min}$ (e^- /Å^3)	0.50 and −0.41	0.84 and −0.48
CSD number	1585756	1585757

Supplementary Table 7: Crystallographic data of crystals containing ephedrinium chloride, bromide and iodide (form II) salts.

name	**[(+)-EphH][chloride]**	**[(+)-EphH][bromide]**	**[(+)-EphH][iodide]**, form II
Empirical formula	$[C_{10}H_{16}CNO]Cl$	$[C_{10}H_{16}NO]Br$	$[C_{10}H_{16}NO]I$
Diffractometer	Synergy	Supernova	Synergy
Wavelength (Å)	0.71073	0.71073	1.54184
mol. weight (g/mol)	201.69	246.15	293.14
Crystal system	monoclinic	monoclinic	monoclinic
Space group	$P2_1$	$P2_1$	$P2_1$
a (Å)	7.2565(3)	7.4467(2)	5.40542(18)
b (Å)	6.1232(3)	6.20961(16)	6.94898(18)
c (Å)	12.5570(6)	12.5863(4)	16.0701(4)
α (°)	90	90	90
β (°)	102.256(5)	101.176(3)	95.864(3)
γ (°)	90	90	90
Volume ($Å^3$)	545.23(4)	570.96(3)	600.47(3)
Z	2	2	2
Density(calc.) (g/cm^3)	1.229	1.432	1.621
Linear abs. coeff. (mm^{-1})	0.314	3.565	20.679
F(000)	216	252	288
Crystal size (mm^3)	0.40 × 0.08 × 0.04	0.41 × 0.07 × 0.05	0.25 × 0.06 × 0.011
Crystal description	colourless needle	needle, colorless	plate, colorless
θ range (°)	2.873; 32.767	2.952; 32.888	5.535; 74.157
Reflections collected	7304	9436	7652
Indep. reflections	3239 [R_{int} = 0.0287]	3804 [R_{int} = 0.0227]	2282 [R_{int} = 0.0330]
Reflections obs.	2969	3388	2164
Criterion for obs.	I > 2.0σ(I)	I > 2.0σ(I)	I > 2.0σ(I)
Completeness to θ (°)	99.8 % to 25.242°	99.8 % to 25.242°	0.978 to 67.684
Absorption corr.	multi-scan	gaussian	gaussian
Min. and max. transm.	0.74501 and 1	0.543 and 1	0.215 and 0.993
Reflections / restraints / parameters	3239 / 1 / 121	3804 / 1 / 121	2282 / 1 / 121
Goodness-of-fit on F^2	1.059	1.045	1.075
Final R ind. [I > 2.0σ(I)]	R_1 = 0.0302 wR_2 = 0.0722	R_1 = 0.0303 wR_2 = 0.0716	R_1 = 0.0254 wR_2 = 0.0629
R indices (all data)	R_1 = 0.0338 wR_2 = 0.0737	R_1 = 0.0380 wR_2 = 0.0749	R_1 = 0.0278 wR_2 = 0.0642
Final $\Delta\rho_{max,min}$ ($e^-/Å^3$)	0.283 and -0.166	0.387 and -0.280	0.30/-0.69
Flack parameter	-0.02(3)	-0.009(5)	-0.018(10)
CSD number	1823199	1823200	1585759

Supplementary Table 8: Crystallographic data of crystals containing ephedrinium iodide (form I), oxalate and thiocyanate salts.

name	**[(+)-EphH][iodide]**, form I	**[(+)-EphH]$_2$[oxalate]**	**[(+)-EphH] thiocyanate**
Empirical formula	$[C_{10}H_{16}NO]I$	$[C_{10}H_{16}NO]_2[C_2O_4]$	$[C_{10}H_{16}NO]SCN$
Diffractometer	Synergy	SuperNova	Synergy
Wavelength (Å)	0.71073	0.71073	1.54184
mol. weight (g/mol)	293.14	420.49	224.32
Crystal system	orthorhombic	monoclinic	orthorhombic
Space group	$P2_12_12_1$	$C2$	$P2_12_12_1$
a (Å)	7.32726(12)	13.5545(2)	6.09862(6)
b (Å)	18.9411(3)	5.84781(7)	7.52704(9)
c (Å)	25.6662(5)	14.1657(2)	27.3811(3)
α (°)	90	90	90
β (°)	90	110.071(2)	90
γ (°)	90	90	90
Volume (Å^3)	3562.12(11)	1054.64(3)	1256.92(2)
Z	12	2	4
Density(calc.) (g/cm^3)	1.64	1.324	1.185
Linear abs. coeff. (mm^{-1})	2.664	0.096	2.107
F(000)	1728	452	480
Crystal size (mm^3)	0.29 × 0.17 × 0.05	0.39 × 0.18 × 0.11	0.16 × 0.14 × 0.010
Crystal description	plate, colorless	prism, colorless	colourless plate
θ range (°)	2.150; 33.484	3.591; 35.243	3.228; 78.698
Reflections collected	88148	20898	10879
Indep. reflections	12569 [R_{int} = 0.0322]	4451 [R_{int} = 0.0255]	2659 [R_{int} = 0.0261]
Reflections obs.	11728	4049	2582
Criterion for obs.	I > 2.0σ(I)	I > 2.0σ(I)	I > 2.0σ(I)
Completeness to θ (°)	0.999 to 25.242	0.996 to 25.242	99.6 % to 67.684°
Absorption corr.	gaussian	gaussian	multi-scan
Min. and max. transm.	0.419 and 1	0.568 and 1	0.82868 and 1
Reflections / restraints / parameters	12569 / 0 / 361	4451 / 1 / 145	2659 / 0 / 139
Goodness-of-fit on F^2	1.067	1.05	1.048
Final R ind. [I > 2.0σ(I)]	R_1 = 0.0225 wR_2 = 0.0472	R_1 = 0.0337 wR_2 = 0.0811	R_1 = 0.0258 wR_2 = 0.0672
R indices (all data)	R_1 = 0.0258 wR_2 = 0.0480	R_1 = 0.0418, wR_2 = 0.0864	R_1 = 0.0267 wR_2 = 0.0676
Final $\Delta\rho_{max,min}$ (e$^-$ /Å^3)	0.92 and -0.898	0.33 and -0.18	0.174 and -0.164
Flack parameter	-0.020(5)	0.2(2)	-0.005(6)
CSD number	1585758	1585760	1823201

Supplementary Table 9: Crystallographic data of crystals containing trazodone

name	**[TrH][iodide]**	**[TrH]$_2$[oxalate]** ·10(H_2O)	**[Tr]**·2(H_2O)
Empirical formula	$[C_{19}H_{23}ClN_5O]I$	$[C_{19}H_{23}ClN_5O]_2$ $[C_2O_4]\cdot 10(H_2O)$	$C_{19}H_{22}ClN_5O$ ·2(H_2O)
Diffractometer	SuperNova	SuperNova	SuperNova
Wavelength (Å)	0.71073	1.54184	1.54184
mol. weight (g/mol)	499.77	1013.92	405.88
Crystal system	monoclinic	monoclinic	monoclinic
Space group	*P*2$_1$/*c*	*I*2/a	*P*2$_1$/c
a (Å)	12.9279(2)	15.1489(4)	7.10113(10)
b (Å)	12.54570(15)	13.2904(4)	13.6250(2)
c (Å)	13.13900(15)	24.5940(8)	20.6821(3)
α (°)	90	90	90
β (°)	109.8430(12)	97.293(3)	91.5054(12)
γ (°)	90	90	90
Volume (Å^3)	2004.48(5)	4911.6(3)	2000.36(5)
Z	4	4	4
Density(calc.) (g/cm^3)	1.656	1.371	1.354
Linear abs. coeff. (mm^{-1})	1.75	1.85	1.948
F(000)	1000	2152	856
Crystal size (mm^3)	0.20 × 0.07 × 0.04	0.14 × 0.07 × 0.04	0.28 × 0.15 × 0.02
Crystal description	plate, colorless	needle, colorless	plate, colorless
θ range (°)	3.248; 33.727	3.624; 76.973	3.886; 74.266
Reflections collected	27961	20149	29860
Indep. reflections	7970 [R_{int} = 0.0340]	5113 [R_{int} = 0.0336]	4036 [R_{int} = 0.0332]
Reflections obs.	6177	4562	3588
Criterion for obs.	I > 2.0σ(I)	I > 2.0σ(I)	I > 2.0σ(I)
Completeness to θ (°)	0.995 to 25.242	1.000 to 67.684	1.000 to 67.684
Absorption corr.	multi-scan	gaussian	multi-scan
Min. and max. transm.	0.649 and 1	0.783 and 1	0.733 and 1
Reflections / restraints / parameters	7970 / 0 / 244	5113 / 6 / 341	4036 / 10 / 337
Goodness-of-fit on F^2	1.025	1.069	1.032
Final R ind. [I > 2.0σ(I)]	R_1 = 0.0336 wR_2 = 0.0626	R_1 = 0.0445 wR_2 = 0.1210	R_1 = 0.0408 wR_2 = 0.1095
R indices (all data)	R_1 = 0.0527 wR_2 = 0.0684	R_1 = 0.0485 wR_2 = 0.1251	R_1 = 0.0456 wR_2 = 0.1143
Final $\Delta\rho_{max,min}$ (e^- /Å^3)	0.71 and -0.45	0.24 and -0.32	0.37 and -0.26
CSD number	1585764	1585765	1585763

References:

1. M. Tiffner, J. Novacek, A. Busillo, K. Gratzer, A. Massa and M. Waser, *RSC Adv.*, 2015, **5**, 78941-78949.
2. A. McPherson and J. A. Gavira, *Acta Cryst.*, 2014, **F70**, 2-20.
3. Rigaku Oxford Diffraction, CrysAlis^{Pro} Software system 1.171.38, Rigaku Corporation, Oxford, UK, 2015.
4. A. Altomare, M. C. Burla, M. Camalli, G. L. Cascarano, C. Giacovazzo, A. Guagliardi, A. G. G. Moliterni, G. Polidori and R. Spagna, *J. Appl. Cryst.*, 1999, **32**, 115-119.
5. L. Palatinus and G. Chapuis, *J. Appl. Cryst.*, 2007, **40**, 786-790.
6. G. M. Sheldrick, *Acta Cryst.*, 2015, **C71**, 3-8.
7. C. B. Hübschle, G. M. Sheldrick and B. Dittrich, *J. Appl. Cryst.*, 2011, **44**, 1281-1284.
8. P. W. Betteridge, J. R. Carruthers, R. I. Cooper, K. Prout and D. J. Watkin, *J. Appl. Cryst.*, 2003, **36**, 1487-1487.
9. C. F. Macrae, I. J. Bruno, J. A. Chisholm, P. R. Edgington, P. McCabe, E. Pidcock, L. Rodriguez-Monge, R. Taylor, J. van de Streek and P. A. Wood, *J. Appl. Cryst.*, 2008, **41**, 466-470.
10. A. V. George, L. D. Field, E. Y. Malouf, A. E. D. McQueen, S. R. Pike, G. R. Purches, T. W. Hambley, I. E. Buys, A. H. White, D. C. R. Hockless and B. W. Skelton, *J. Organomet. Chem.*, 1997, **538**, 101-110.
11. A. Rodriguez-Fortea, P. Alemany, S. Alvarez, E. Ruiz, A. Scuiller, C. Decroix, V. Marvaud, J. Vaissermann, M. Verdaguer, I. Rosenman and M. Julve, *Inorg. Chem.*, 2001, **40**, 5868-5877.
12. A. Peuronen, E. Lehtimäki and M. Lahtinen, *Cryst. Growth Des.*, 2013, **13**, 4615-4622.
13. E. A. Collier, R. J. Davey, S. N. Black and R. J. Roberts, *Acta Cryst.*, 2006, **B62**, 498-505.
14. B. Gossner and H. Neff, *Z. Kristallogr.*, 1933, **86**, 32-41.
15. K. Schwantke, *Z. Kristallogr.*, 1909, **46**, 73-115.
16. A. L. Spek, *J. Appl. Cryst.*, 2003, **36**, 7-13.
17. R. W. W. Hooft, L. H. Straver and A. L. Spek, *J. Appl. Cryst.*, 2008, **41**, 96-103.